Drosophila p38 MAPK Interacts with BAG-3/starvin to Regulate Age-dependent Protein Homeostasis

Sarah M. Ryan[2,*], Michael Almassey[1,*], Amelia M. Burch[3], Gia Ngo[2], Julia M. Martin[1], David Myers[1], Devin Compton[1], Scott Barbee[2], Nathan T. Mortimer[1], Subhabrata Sanyal[3,4] and Alysia D. Vrailas-Mortimer[1-3]

1 Illinois State University, School of Biological Sciences, Normal, IL, USA

2 University of Denver, Department of Biological Sciences, Denver, CO, USA

3 Emory University, Department of Cell Biology, Atlanta, GA, USA

4 Calico, San Francisco, CA, USA

Running Title: p38K Regulates Age-Dependent Proteostasis

Key words/phrases: p38 MAPK, BAG-3/starvin, protein aggregation, aging, Lamin

Corresponding author:
Alysia D. Vrailas-Mortimer
Illinois State University
School of Biological Sciences
Science Laboratory Building
Normal, IL 61790
Phone: 309-348-8574
Fax: 309-348-3722
e-mail: admorti@ilstu.edu

53

54 **Summary**

55

56 As organisms age, they often accumulate protein aggregates that are thought to be
57 toxic, potentially leading to age-related diseases. This accumulation of protein
58 aggregates is partially attributed to a failure to maintain protein homeostasis. A variety of
59 genetic factors have been linked to longevity, but how these factors also contribute to
60 protein homeostasis is not completely understood. In order to understand the
61 relationship between aging and protein aggregation, we tested how a gene that
62 regulates lifespan and age-dependent locomotor behaviors, p38 MAPK (p38Kb),
63 influences protein homeostasis as an organism ages. We find that p38Kb regulates age-
64 dependent protein aggregation through an interaction with the Chaperone-Assisted
65 Selective Autophagy complex. Furthermore, we have identified Lamin as an age-
66 dependent target of p38Kb and the Chaperone-Assisted Selective Autophagy complex.

67

68 **Introduction**

69

70 Protein turnover is critical for maintaining tissue health as many proteins become
71 damaged or misfolded during normal tissue functions. Therefore, the cell utilizes a
72 variety of protein quality control mechanisms to refold or degrade these damaged
73 proteins, including the ubiquitin proteasome system and macroautophagy. During aging,
74 protein quality control mechanisms become less efficient leading to the accumulation of
75 damaged or misfolded proteins that begin to form protein aggregates[1]. It has been
76 hypothesized that these aggregates are toxic and may lead to the deleterious
77 phenotypes associated with normal aging, such as impaired tissue function[1].
78 Furthermore, decreased protein aggregation has been associated with longevity. For

79 example, over-expression of Foxo leads to an increased lifespan but also a concordant
80 decrease in protein aggregation in *C. elegans*, *Drosophila,* and mice [2–6], suggesting that
81 lifespan and protein aggregation are tightly linked processes. However, the molecular
82 mechanisms that underlie the relationship between aging and protein homeostasis have
83 not been fully characterized.
84
85 One pathway that has been linked to both aging and protein homeostasis is the
86 stress response p38 MAPK (p38K) pathway. In mammals, there are four p38K genes (α,
87 β, γ, and δ), and p38Kα has been linked to both the inhibition [7,8] and induction [9,10] of
88 macroautophagy, in particular in response to oxidative stress [11,12]. In addition, p38Kα
89 has been linked to regulating macroautophagy in cellular senescence [13–15]. However,
90 how p38K signaling may contribute to protein homeostasis in response to natural aging
91 is not well understood. The fruit fly *Drosophila melanogaster* has two canonical p38K
92 genes (p38Ka and p38Kb), and we have previously reported that p38Kb acts in the adult
93 musculature to regulate aging. We found that over-expression of p38Kb leads to
94 increased lifespan while loss of p38Kb results in a short lifespan and age-dependent
95 locomotor behavior defects [16]. In addition, oxidatively damaged proteins accumulate in
96 the muscle of p38Kb mutants with age [16], and loss of p38Kb leads to increased
97 polyubiquitination of insoluble proteins and alterations in oxidative stress dependent
98 translation [17], suggesting that these oxidatively damaged proteins may be aggregating in
99 p38Kb mutants. Furthermore, p38Kb has been shown in a *Drosophila* cell culture system
100 to pull down with the HspB8 homologue CG14207 [18], which plays a role in the muscle by
101 regulating protein homeostasis as a part of a protein quality control mechanism called
102 BAG-3 Mediated Selective Macroautophagy pathway in mammalian systems or the
103 Chaperone-Assisted Selective Autophagy (CASA) complex in flies [19,20]. The CASA
104 complex also includes the chaperone Hsc70 and the co-chaperone BAG-3 (starvin in

flies). BAG-3/starvin binds to specific damaged or misfolded protein substrates and brings them to the CASA complex where it binds to Hsc70 and HspB8. Those substrates that cannot be refolded by the complex are polyubiquitinated and targeted to the autophagosome through a handover between BAG-3/stv and the autophagy adaptor protein p62 (ref(2)p in flies), and subsequently degraded through the autophagosome-lysosome system [21–25].

Here, we report that p38Kb regulates age-dependent muscle protein homeostasis through an interaction with the CASA complex. We find that p38Kb acts as an intermediary between BAG-3/starvin and p62/ref(2)p in targeting damaged or misfolded proteins for degradation. This interaction is not only important for maintaining protein homeostasis but also for lifespan extension. In addition, we find that the *Drosophila* homologue of the Hutchinson-Gilford progeria protein, Lamin A/C, is a target for p38Kb and CASA complex mediated protein turnover, suggesting that the p38Kb aging phenotypes may be a result of impaired Lamin degradation.

Materials and Methods

Genotypes

UAS-p38Kb wt, UAS-p38Kb Kinase Dead, p38Kb$^{\Delta 45}$, p38Kb^{Ex41}, w^{1118}, Mef2-GAL4 and MHC-GAL4 were as described in [16]. The p38Kb^{Ex41} is a precise excision allele and serves as a genetic background control for p38Kb$^{\Delta 45}$ deletion mutation.

129 UAS-stv RNAi 34408 (w^{1118}; P{GD10796}v34408) and UAS-stv RNAi 34409 (w^{1118};
130 P{GD10796}v34409/TM3) are described in [26] and are from the Vienna Drosophila
131 Resource Center.
132
133 stv-GFP trap (w^{11118};; Pbac{754.P.F3v30} $stv^{+CPTI\ 002824}$), HspB8-GFP trap (w^{1118}
134 PBac{810.P.FSVS-2}$CG14207^{CPTI004445}$), Hsc70-4 GFP trap (*w^{1118} PBac{544.SVS-*
135 *1}$N^{CPTI002347}$*) are from the Kyoto Stock Center.
136
137 w^{1118}; P{y[+mDint2] w[BR.E.BR]=SUPor-P}ref(2)$P^{KG00926}$, w^{1118};;+mDint2 EY4969 stvEP,
138 Lam^{A25} pr^{1}, P{UAS-mito-HA-GFP.AP}3, w[126]; P{w[+mC]=UAS-Hsc70-4.WT}B, and
139 w^{1118}; P{w[+mC]=UAS-Lam.GFP}3-3 were obtained from the Bloomington Drosophila
140 Stock Center.
141
142 All fly stocks were backcrossed into the w^{1118} background and isogenized for 10
143 generations. All stocks were reared at 25ºC in a 12hr:12hr light:dark cycle on standard
144 fly food media.
145
146 **Immunofluorescence**
147 Adult flies were fixed in 4% paraformaldehyde for 48hrs at 4°C. Indirect flight muscles
148 were dissected in 1X PBS, permeabilized in 1X PBS 0.15% Triton-X 100, and blocked in
149 NGS + 0.15% Triton-X 100. Samples were incubated in primary antibody at 4°C
150 overnight, washed in 1X PBS 0.15% Triton-X 100, and incubated in secondary antibody
151 at room temperature for 2hrs. Samples were mounted in Vectashield mounting medium
152 (Vectorlabs) and visualized using a laser scanning confocal microscope. Antibodies:
153 rabbit anti-GFP 1:400 (Invitrogen), mouse anti-FLAG M2 1:1000 (Sigma), rabbit anti-stv
154 1:1000 (gift of Jög Höhfeld), rat anti-α actinin 1:100 (Abcam), rabbit anti-ubiquitin

155 linkage-specific K63 anti-mouse 1:200 (Abcam), IgG- Alexa Fluor 488 1:200 (Life
156 Technologies), anti-mouse IgG- Alexa Fluor 568 1:500 (Life Technologies), anti-rabbit
157 IgG- Alexa Fluor 488 1:500 (Life Technologies) and Rhodamine Phalloidin 1:2000.
158

159 **Protein aggregate analysis**

160 Indirect flight muscles were prepared as described above from 9 individual flies per
161 genotype. Protein aggregates were identified using mouse anti-polyubiquitin 1:1000
162 (Enzo Life Sciences). Three muscles from each individual fly were imaged as z-series
163 and flattened into a single image as a max projection using confocal microscopy for a
164 total of 27 muscles per genotype. Images were analyzed using Image J "Analyze
165 Particles" function with a diameter of 100 pixels set for the minimum aggregate size.
166 Aggregate number and size were analyzed using ANOVA followed by Tukey's HSD
167 using the R package "multcomp" to generate significance groups with each letter group
168 being significantly different with a p value of ≤ 0.05. Within genotype/across time point
169 analyses were performed using the Welch two sample t-test in R.
170

171 **Lifespan**

172 For lifespan experiments using the UAS-p38Kb^{wt}, ref(2)p -/+, p38Kb$^{\Delta 45/\Delta 45}$, the stv EP
173 (stv^{wt}) lines, and their respective controls, virgin females were kept on standard
174 molasses *Drosophila* media. Due to a change in lab food, the stv RNAi 34408 and stv
175 RNAi 34409 lifespan experiments (with their respective controls) were performed on the
176 standard Bloomington *Drosophila* media. Virgin flies were collected and reared at 25°C
177 in a 12hour:12hour light:dark cycle. Flies were put on new food twice a week. The
178 number of dead animals was scored daily. Lifespan was analyzed using a log rank test
179 to compare genotypes with censored data on all genotypes and then on all pairwise

180 comparisons using the R package “survival” with Benjamini and Hochberg correction
181 (false discovery rate < 0.05).
182
183 **Co-immunoprecipitation**
184 Flies were aged 1 week or 5 weeks. Forty thoraxes per genotype per condition were
185 homogenized in high salt buffer (0.5 M KCl, 35% glycerol,10 mM HEPES pH 7.0, 5 mM
186 $MgCl_2$, 0.5 mM EDTA pH 8.0, 0.1% NP40 25 mM NaF, 1 mM Na_2VO_4, 1 mM DTT,
187 Complete protease inhibitor). The lysate was flash frozen in liquid nitrogen and quickly
188 thawed at 37°C. Then lysates were rocked at 4°C for 30 minutes and centrifuged at
189 14,200 x g for 30 minutes at 4°C. The supernatant was transferred to equilibrated beads
190 anti-Flag (M2) agarose (Sigma) or anti-GFP agarose (Chromotek) and rocked for 2
191 hours at 4°C. Beads were collected using a magnetic bar and washed four times with IP
192 buffer (50 mM HEPES pH 7.0, 100 mM KCl, 0.4% NP40 1.5 mM $MgCl_2$, 5% glycerol, 25
193 mM Na, 1 mM Na_2VO_4, 1 mM EDTA, 1 mM DTT, Complete protease inhibitor). Lysates
194 were then analyzed by immunoblotting using rabbit anti- GFP 1:1000 (Invitrogen),
195 mouse anti-FLAG M2 1:1000 (Sigma), rabbit anti-phospho-p38 1:1000 (Cell Signaling
196 Technologies), goat anti total p38 1:1000 (Santa Cruz Biotechnology), rabbit anti-stv
197 1:10,000 (gift of Jrög Höhfeld) or mouse anti-Lamin 1:1000 (DHSB).
198
199 **Immunoblotting**
200 Wild type flies (w^{1118}) were aged either for 3, 15, 30, and 45 days or for 1-5 weeks. Three
201 thoraxes were dissected and homogenized in 1x Laemmli buffer. Immunoblots were
202 performed as described in [16]. Membranes were developed using SuperSignal West
203 Femto kit (ThermoFisher) or Pierce ECL (ThermoFisher) and exposed on
204 autoradiography film. Antibodies used were: rabbit anti-GFP 1:1000 (Invitrogen), rabbit

205 anti-starvin 1:10,000 (gift of Jrög Höhfeld), mouse anti-actin 1:5,000,000 (Sigma), mouse
206 anti-FLAG M2 (Sigma), rabbit anti-alpha tubulin (Cell Signaling Technologies), mouse
207 anti-Lamin 1:100 (DHSB), rabbit anti-phospho Lamin A Ser22 1:1000 (Thermofisher),
208 mouse anti-beta tubulin (E-10) 1:5000 (Santa Cruz Biotechnology), mouse anti- HRP
209 1:20,000 (Jackson Labs), rabbit anti-HRP 1:40,000 (Jackson Labs). Densitometry was
210 performed using a minimum of three independent blots. For statistical analysis of protein
211 expression level, pixel density of the tested protein was normalized within sample to the
212 loading control. These values were then normalized to control to calculate fold change.
213 The fold change values were analyzed by Student's t-test or ANOVA [27] as appropriate.
214

215 **Sucrose Gradient Fractionation**

216 $p38Kb^{Ex41/Ex41}$ and $p38Kb^{\Delta45/\Delta45}$ flies were aged three weeks. 30 thoraxes per genotype
217 were dissected and homogenized in NP40 lysis buffer. Samples were centrifuged at
218 800xg for 10 minutes at 4°C. The supernatant was then transferred to a 15-50% sucrose
219 discontinuous gradient. Samples were then ultracentrifuged at 55,000 rpm (201,000xg at
220 r_{av}) for 20 hours at 4°C in a TLS-55 in a Beckman Coulter Optima TLX Ultracentrifuge.
221 200μl fractions were collected and the pellet was resuspended in an equal volume of
222 NP40 Lysis Buffer.
223

224 **Stv localization**

225 Immunohistochemistry on $p38Kb^{Ex41/ Ex41}$ and $p38Kb^{\Delta45/\Delta45}$ Indirect flight muscles was
226 performed as described above. Confocal images from five individual flies per genoytpe
227 were analyzed for average pixel density using ImageJ in three different non-overlapping
228 locations on each muscle for a total of 15 measurements per genotype. Average pixel
229 density was analyzed by Student's t-test using R.
230

231 **Results**

232

233 **p38Kb regulates age-dependent protein homeostasis.**

234 p38Kb null mutant animals (p38Kb$^{\Delta45/\Delta45}$, a deletion of the p38Kb gene) exhibit age-
235 dependent locomotor behavior defects and have a 48% lifespan reduction. In addition,
236 biochemical analysis suggests that p38Kb null mutants have increased levels of
237 insoluble polyubiquitinated proteins in the thoracic musculature of aged animals as
238 observed by immunoblot analysis [17]. However, protein aggregate size and distribution
239 have not been visualized in the p38Kb mutants, nor is it known whether augmenting
240 p38Kb activity in muscles leads to a change in protein homeostasis. Therefore, we
241 analyzed how p38Kb expression influences protein aggregation. We find that p38Kb null
242 mutants have an increased number of protein aggregates in the adult indirect flight
243 muscle at 1 week and 3 weeks of age (Figure 1A-B and E-F, Table S1) and increased
244 aggregate size with age (Figure 1G-H, Table S1) as compared to a genetic background
245 control (p38Kb$^{Ex41/Ex41}$, a precise excision allele). Furthermore, transgenic inhibition of
246 p38Kb in the muscle using a dominant negative kinase dead construct (p38Kb^{KD}, [16]) also
247 results in a significant increase in aggregate number, however aggregate size was not
248 affected (Figure 1I-L and Table S2). Conversely, as both strong and moderate levels of
249 p38Kb over-expression lead to an increased lifespan (37% and 14% extension,
250 respectively) [16], we tested if p38Kb over-expression also affects protein aggregation. We
251 find that both strong over-expression of p38Kb in the adult muscle using the Mef2-GAL4
252 driver (Figure 1C-D and M-P, Table S3) and moderate over-expression of p38Kb using
253 the MHC-GAL4 driver (Figure 1Q-T and Table S4) leads to decreased protein aggregate
254 number and size throughout the lifespan. It has been hypothesized that protein
255 aggregate accumulation and increased size may be toxic, potentially explaining the

256 decreased lifespan and age-dependent locomotor abnormalities in p38Kb$^{\Delta 45}$ null mutants
257 and the increased longevity in the p38Kb over-expression animals.
258
259 **p38Kb mediates age-dependent phenotypes through autophagy**
260 In order to determine what mechanism plays a role in the clearance of polyubiquitinated
261 protein aggregates, we first tested what type of ubiquitin linkage is present in the
262 aggregates in wild type flies. In particular, K63-linked ubiquitination has been shown to
263 facilitate the formation of aggregates [28–30] that are cleared through autophagy [30–32]. We
264 find that a subset of aggregates from both aged wild type and p38Kb mutant flies contain
265 K63-linked ubiquitinated proteins (Figure 2), suggesting that these muscle protein
266 aggregates are degraded through autophagy.
267
268 Polyubiquitinated protein aggregates can be degraded through selective
269 autophagy in which the adaptor protein p62 (ref(2)p in flies) promotes the packaging and
270 delivery of polyubiquitinated proteins to the autophagosome[33]. If p38Kb requires
271 selective autophagy to mediate protein homeostasis, then loss of ref(2)p will block the
272 p38Kb mediated decreased aggregation phenotype. We find that loss of a single copy of
273 *ref(2)p* results in fewer aggregates (Figure 2G-H and Table S5), which may reflect
274 compensation by other protein clearance mechanisms with aging, especially as
275 homozygous *ref(2)p* mutants are viable. When a single copy of *ref(2)p* is removed in the
276 p38Kb over-expression background, this prevents the reduced protein aggregation
277 observed in the p38Kb over-expression animals at both young and old ages (Figure 2G-
278 H and Table S5). This dominant interaction suggests that *ref(2)p* acts downstream of
279 p38Kb to promote the degradation of protein aggregates.
280
281 **p38Kb colocalizes with the CASA complex in the adult flight muscle.**

282 In order to better understand the role of p38Kb in protein homeostasis, we first
283 determined where in the muscle p38Kb localizes and find that a FLAG-tagged p38Kb
284 (green) colocalizes with the Z-disc marker alpha-actinin and is also present at the M-line
285 (Figure 3A). The muscle Z-disc is an area of high protein turnover, and one protein
286 quality control mechanism that localizes to the Z-disc in mice and adult flies is the
287 Chaperone-Assisted Selective Autophagy (CASA) complex (known as the BAG-3
288 mediated selective autophagy complex in mammals)[19,34,35]. In adult *Drosophila* muscle,
289 the CASA complex has been reported to consist of the Hsc70 homologue Hsc70-4, the
290 HspB8 homologue CG14207 and the BAG-3 homologue starvin (stv) [19]. We find that
291 p38Kb colocalizes with all the CASA complex members at the Z-disc and M-line (Figure
292 3B-D).
293
294 **p38Kb physically interacts with the CASA complex in the adult flight muscle.**
295 In order to further determine if p38Kb physically interacts with the CASA complex in the
296 adult muscle, we performed co-immunoprecipitation experiments. In *Drosophila* cell
297 culture p38Kb^{wt} was shown to co-immunoprecipitate with the HspB8 homologue
298 CG14207[18], therefore, we tested if this interaction also occurs in adult indirect flight
299 muscle. As the interaction between p38Kb and its targets may be transient, we utilized a
300 FLAG-tagged p38Kb kinase dead construct (UAS-p38Kb^{KD} Mef2-GAL4) that is able to
301 be activated and bind to a target but cannot phosphorylate it, leading to a delayed
302 release of the target[36]. We expressed p38Kb^{KD} in the adult flight muscle of a fly that also
303 endogenously expressed GFP tagged HspB8, in which GFP is spliced in as a new exon
304 of the endogenous gene. This results in a GFP fusion protein that is expressed in the
305 same pattern as endogenous HspB8 ([19] and Figure 3C'). We find that p38Kb^{KD} was able
306 to pull down HspB8 (Figure 3E) as compared to the HspB8-GFP control background. In
307 addition, expression of p38Kb^{KD} in a wildtype background was able to pull down un-

308 tagged endogenous stv (Figure 3F). We then performed the reverse
309 immunoprecipitation experiments in which we immunoprecipitated control GFP or
310 endogenously GFP tagged Hsc70-4, HspB8 or stv from muscle lysates and probed for
311 endogenous phosphorylated p38K, which is the active form of p38K. We find that all
312 three members of the CASA can co-immunoprecipitate with endogenous phosphorylated
313 p38K in the muscle (Figure 3G, Figure S1D). We repeated these experiments in which
314 we expressed the FLAG tagged p38Kb^{KD} and found that p38Kb co-immunoprecipitates
315 with the CASA complex (Figure S1A-C) with stronger binding at younger ages than older
316 ages. To determine if this reduction in binding was due to an age-dependent decrease in
317 the ability of p38K to associate with the CASA complex, we tested if the expression
318 levels of either the CASA complex or the FLAG tagged p38Kb^{KD} are changed with age.
319 We found no significant difference in the expression levels of Hsc70-GFP and stv-GFP
320 with age (Figure S2A and C) while levels of HspB8-GFP increased with age (Figure
321 S2B). In addition, the levels of over-expressed p38Kb^{KD} declined with age (Figure S2D).
322 We also have found that levels of p38K decline with age[37]. These data suggest that the
323 levels of p38Kb protein may be limiting for CASA complex functions as the fly ages.
324
325 **p38Kb acts downstream of the CASA complex.**
326 We next tested the relationship between p38Kb and the CASA complex to
327 determine if p38Kb acts either upstream or downstream of the CASA complex to
328 promote protein homeostasis. As BAG-3/stv provides both the specificity to the CASA
329 complex and is involved in the handoff of damaged proteins to p62/ref(2)p for autosomal
330 degradation [21–25], we tested for genetic interactions between p38Kb and *stv*. *stv* null
331 mutants have impaired locomotor functions, muscle degeneration and early lethality [19,38].
332 Due to the severity of these null phenotypes, we utilized *stv* RNAi lines to generate an
333 allelic series of *stv* loss of function in the muscle. We find that weak inhibition of stv

334 (UAS-stv RNAi^{34408} MHC-GAL4) had no effect on protein aggregation (Table S6).
335 However, moderate inhibition of stv (UAS-stv RNAi^{34409} MHC-GAL4) results in increased
336 protein aggregate number and size (Figure 4A-B and Table S7) and results in a
337 decrease in lifespan particularly in the first half of life as compared to outcrossed
338 controls (Figure 4C and Table S8). Strong inhibition of *stv* (UAS-stv RNAi^{34408} Mef2-
339 GAL4) leads to a severely reduced lifespan of ~4 days on average (Figure 4D and Table
340 S9).
341
342 If p38Kb acts to regulate the downstream activity of the CASA complex, then
343 over-expression of p38Kb should rescue these *stv* RNAi phenotypes. We find that over-
344 expression of p38Kb rescues both protein aggregate number and size in the *stv*
345 moderate inhibition background (Figure 4A-B and Table S7) and also rescues the
346 lifespan defect (Figure 4C and Table S8). Furthermore, p38Kb over-expression is able to
347 partially rescue the decreased lifespan exhibited by strong *stv* inhibition increasing
348 average lifespan from 4 days to 13 days (Figure 4D and Table S9). To further test if
349 p38Kb acts downstream of the CASA complex, we combined loss of p38Kb with CASA
350 complex over-expression. If p38Kb acts downstream of the CASA complex, then over-
351 expression of the CASA complex members in the p38Kb mutant background will not be
352 able to rescue the p38Kb mutant phenotypes. We find that over-expression of Hsc70-4
353 in the muscle fails to rescue the p38Kb mutant shortened lifespan (Figure S3A, Table
354 S10), even though this extends lifespan in a wild type background (Figure S3B, Table
355 S11). Furthermore, we find that over-expression of stv in the p38Kb mutants not only
356 fails to rescue the p38Kb mediated short lifespan defect but reduces the lifespan further
357 (Figure 4E and Table S12). This is particularly striking as over-expression of stv in a wild
358 type background does not significantly affect lifespan (Figure 5E and Table S13) as
359 compared to the outcrossed transgene control. These data in combination with the

360 decrease of p38K binding to the CASA complex with age when p38K levels are reduced
361 suggest that p38Kb may be a limiting factor in regulating the downstream activity of the
362 CASA complex in which it hands the poly-ubiquitinated misfolded proteins to ref(2)p for
363 degradation through the autophagosome.
364
365 **p38Kb regulates the activity of the CASA complex in protein homeostasis.**
366 If p38Kb is a limiting factor for stv function, then the combined over-expression of
367 p38Kb and stv may result in a further beneficial effect. We find that over-expression of
368 stv alone results in fewer aggregates at young and old ages (Figure 5A-B and Table
369 S14) and smaller aggregates with age (Figure 5D and Table S14) as compared to
370 outcrossed controls. However, co-over-expression of p38Kb and stv does not result in a
371 further reduction in aggregate number as compared to over-expression of p38Kb or stv
372 alone (Figure 5A and Table S14). By 5 weeks of age, co-over-expression of p38Kb and
373 stv flies have comparable aggregate number to controls (Figure 5B and Table S14).
374 Conversely, p38Kb and stv co-over-expression results in a reduction in aggregate size at
375 a young age compared to over-expression of stv alone (Figure 5C and Table S14),
376 suggesting that p38Kb is a limiting factor for stv function in regulating aggregate size.
377 Unlike with aggregate number, the aggregates remain significantly smaller in size as the
378 flies age in the combined over-expression background (Figure 5D and Table S14). We
379 also find that co-over-expression of p38Kb and stv leads to an additional 5% increase in
380 lifespan relative to p38Kb over-expression alone (Figure 5E and Table S13).
381 Interestingly, the co-over-expression animals show a very similar lifespan to the p38Kb
382 over-expression alone animals until ~day 50, when the p38Kb alone animals begin to die
383 at a faster rate (Figure 5E). These data suggest that co-over-expression of p38Kb and
384 stv provides beneficial effects in early adulthood that continue throughout adulthood
385 leading to increased lifespan despite the presence of protein aggregates. Another

386 possibility is that aggregate size and/or content may play a more important role in
387 determining lifespan as compared to overall aggregate number.
388
389 **p38Kb is required for proper localization of stv in the muscle.**
390 Since we find that p38Kb acts between stv and ref(2)p in regulating protein
391 aggregation, we hypothesize that p38Kb plays a role in stabilizing the transfer of
392 misfolded proteins primed for degradation from the CASA complex to ref(2)p. In support
393 of this hypothesis, we find that over-expression of p38Kb leads to increased efficiency in
394 targeting misfolded proteins to the autophagosome (Figure 1M-T), while inhibition of
395 p38Kb results in increased protein aggregation (Figure 1E-L). In addition, loss of p38Kb
396 may lead to a failure of stv to maintain its interaction with the CASA complex or to
397 interact with ref(2)p. Therefore, we tested if stv is still able to localize to the Z-disc in the
398 absence of p38Kb. We find that in p38Kb null mutants, stv protein levels are increased
399 (Figure 5F), and stv is more diffusely located throughout the muscle but is still able to
400 localize to the Z-disc and M-line in (Figure 5G-I), suggesting that its localization is
401 partially impaired in the absence of p38Kb. Furthermore, we find that the localization of
402 the CASA complex member HspB8 in the muscle is unaffected by loss of p38Kb (Figure
403 S3C-D). These data indicate that p38Kb may play a role in stabilizing the interaction
404 between the CASA complex and stv that allows stv to direct misfolded proteins to
405 ref(2)p.
406
407 **Lamin protein binds to the CASA complex and accumulates in stv RNAi and**
408 **p38Kb mutants.**
409 In order to determine if p38Kb might be playing a role in the targeting of
410 misfolded proteins from stv to ref(2)p, we first needed to identify a protein target of both
411 stv and p38Kb. Therefore, we focused on proteins associated with Limb-Girdle Muscular

412 Dystrophy (LGMD), which is caused by mutations in either BAG-3 (stv, myofibrillar
413 myopathy-6) or HspB8 (LGMD Type 1D) [39–41]. In addition, p38K signaling has been
414 implicated in LGMD [42–44]. *Drosophila* have 19 orthologues of LGMD proteins, one of
415 which is Lamin A/C (Lamin or Lamin Dm0 in flies). Lamin is of particular interest since
416 mutations in Lamin A/C also result in the accelerated aging disorder Hutchinson-Gilford
417 progeria [45–47], and Lamin has been shown to aggregate under oxidative stress conditions
418 [48]. Mutations in Lamin A/C are also sufficient to induce Lamin aggregation and abnormal
419 nuclear morphology in human cell culture, *C. elegans*, and *Drosophila* systems [46,49–57]. In
420 addition, Lamin proteins are highly post-translationally modified, resulting in changes in
421 its solubility[56,58–63]. Furthermore, in *Drosophila* inhibition of either fly homologue of Lamin
422 A/C have similar phenotypes to p38Kb and/or stv mutants, such as reduced locomotor
423 function and increased activity of the Nrf-2/Keap-1 pathway [51,64,6557,66]. In addition, it has
424 recently been shown that BAG-3, one of the mammalian homologues of stv, can target
425 nuclear Lamin B, a paralogue of Lamin A/C, for degradation [67].

426 If Lamin is a target of the CASA complex, then decreased activity of the CASA
427 complex should result in an accumulation of Lamin protein. Flies have two homologues
428 of Lamin A/C, Lamin Dm_0 and LamC. We find that the levels of Lamin Dm_0, do not
429 change with age (Figure 6A), however, inhibition of stv results in a significant increase in
430 the total amount of Lamin Dm_0 protein regardless of age (Figure 6A-B). Interestingly,
431 loss of p38Kb leads to an age-dependent increase in Lamin Dm_0 protein as compared to
432 age matched controls (Figure 6C-D). These data in addition to our findings that p38Kb is
433 limiting for stv localization (Figure 5H) and that the levels of p38Kb decline with age[37]
434 suggest that p38Kb activity later in life is important for maintaining protein homeostasis
435 and lifespan.

436 To investigate if Lamin Dm_0 is accumulating in the protein aggregates, we
437 performed fractionation experiments in which we find that in controls Lamin Dm_0 is

438 predominantly found in fractions 5-7 and also in the aggregate containing pellet (Figure
439 7A), which is characterized by an increased amount of poly-ubiquitinate proteins (Figure
440 7C). Interestingly, we also find a low molecular weight from of Lamin Dm_0 mainly
441 restricted to fraction 5 and a higher molecular weight form that is predominantly in the
442 pellet (Figure 7A). We next tested how loss of p38Kb affects the aggregation of Lamin
443 Dm_0 and find that p38Kb mutants have decreased Lamin Dm_0 in fractions 5-7 with a
444 concurrent increase of both the main and high molecular weight species of Lamin Dm_0 in
445 the pellet (Figure 7A). This suggests that Lamin Dm_0 is a target of p38Kb and that loss of
446 p38Kb results in increased aggregation of Lamin Dm_0.
447
448 Of interest is this high molecular weight form of Lamin Dm_0, which is present in
449 the aggregates (Figure 7A). Lamin proteins are highly post-translationally modified[56,58–
450 63], and one important protein domain in Lamins is the CaaX box, which is farnesylated
451 and required for Lamin localization to the inner nuclear membrane[63,68–70]. To test if this
452 might be a farnesylated form of Lamin Dm_0, we utilized the Lam^{A25} mutant which has a
453 frameshift that results in the loss of the C-terminal CaaX box[71]. We find that the high
454 molecular weight form of Lamin Dm_0 is lost in the Lam^{A25} mutant whereas the
455 predominant 75kDa band of Lamin Dm_0 is still present (Figure 7D). These data suggest
456 that the high molecular weight Lamin Dm_0 we observe is the farnesylated form. We do
457 not observe a consistent effect on levels due to either stv inhibition or loss of p38Kb,
458 which suggest that p38Kb mediates farnesylated Lamin Dm_0 aggregation than overall
459 levels.
460
461 In addition to farnesylation, Lamins can also be phosphorylated by a variety of
462 kinases that can change the solubility of Lamin porteins[56,72]. For example, in a
463 *Drosophila* cell culture system, a phospho-mimic mutation at Ser45 (the equivalent of

464 Ser22 in humans) results in Lamin aggregation in both the nucleus and cytoplasm [56].
465 This serine residue is phosphorylated by the cd2 kinase [73], but is also a predicted p38K
466 phosphorylation site. As the antibody epitope is conserved in both Lam Dm_0 and LamC,
467 we may not be able to detect specific changes in phosphorylated Lam Dm_0 versus
468 LamC, however, we can assess changes in the levels of Lamin phosphorylation in
469 general. We find that phospho-Lamin levels are not significantly altered in the p38Kb
470 mutants (Figure 6E-F), suggesting that p38Kb is not required for Ser45 phosphorylation.
471 Furthermore, this phosphorylated form of Lamin runs at lower molecular weight than the
472 main form of Lamin (Figure 7D top and middle panels), suggesting that Lamins in adult
473 *Drosophila* muscle is further processed. As this phosphorylation site is near the epitope
474 recognized by the total lamin antibody, it maybe that lamin phosphorylation obscures the
475 ability of this antibody to detect this form of Lamin.
476 We next examined if phosphorylated Lamin is also present in the aggregates. We
477 find that in controls, phosphorylated Lamin is present in factions 5-7 with low amounts in
478 the pellet (Figure 7B). We also observe a low molecular weight phospho-Lamin form that
479 appears in the pellet (Figure 7B). In the p38Kb mutants, phospho-Lamin expression is
480 reduced in fractions 6 and 7 and accumulates in the pellet (Figure 7B). Furthermore,
481 increasingly smaller low molecular weight species of phospho-Lamin are present in the
482 $p38Kb^{\Delta 45}$ mutants including the pellet (Figure 7B), suggesting that loss of p38Kb
483 prevents the effective clearance of these Lamin cleavage forms. Interestingly, loss of the
484 Lamin CaaX box does not affect the formation of these lower molecular weight forms,
485 however, it does result in an increase in the phosphorylation of full-length Lamin (Figure
486 7D). Additionally, we do not detect phosphorylation positive high molecular weight forms
487 of Lamin (Figure 7D), suggesting that farnesylated Lamin is not phosphorylated at
488 Ser45. Overall these data suggest that Lamin is processed in a variety of different ways

489 in the adult muscle and these different forms are prone to aggregation in the absence of
490 p38Kb.
491
492 To determine if Lamin Dm_0 is a direct target of p38Kb and the CASA complex, we
493 tested if Lamin Dm_0 can bind to the CASA complex. We immunoprecipitated
494 endogenously GFP tagged HspB8, Hsc70-4 and stv from adult *Drosophila* muscle and
495 probed for endogenous Lamin Dm_0. We find that full-length Lamin Dm_0 co-
496 immunoprecipitates with all three members of the CASA complex (Figure 3G and Figure
497 S1E), but do not detect binding with either the higher or lower molecular weight forms of
498 Lamin Dm_0 found in the fractions (Figure 7A and B). Furthermore, we expressed Lamin
499 Dm_0 tagged with GFP in the muscle and found that endogenous stv co-
500 immunoprecipitates with Lamin Dm_0 (Figure 3G and Figure S1F). These data suggest
501 that the CASA complex is able to bind to full-length Lamin Dm_0 for targeting to the
502 autophagosome.
503
504 As we hypothesize that p38Kb is interacting with the CASA complex at the point
505 in which the poly-ubiquitinated misfolded targets are handed over to ref(2)p for
506 degradation, we tested if p38Kb also binds to Lamin Dm_0. We find that $p38Kb^{KD}$
507 expressed in the muscle co-immunoprecipitates with both high and low molecular weight
508 forms of Lamin Dm_0 (Figure 6G). Interestingly, p38Kb physically interacts with the
509 aggregate prone low molecular weight species of Lamin Dm_0 as opposed to the
510 predominant full-length form of Lamin Dm_0 (Figure 6G). More striking is that $p38Kb^{KD}$
511 physically interacts with increasingly larger forms of Lamin Dm_0 (Figure 6G), suggesting
512 that p38Kb is interacting with the poly-ubiquitinated forms of Lamin Dm_0. Furthermore,
513 we have expressed GFP-tagged Lamin Dm_0 in the muscle and were able to pull down
514 phosphorylated p38K (Figure 3G). These data indicate that p38Kb activation may be

515 important for the hand off of misfolded proteins that are tagged for lysosomal
516 degradation from stv to ref(2)p.
517
518 We have developed a model in which misfolded proteins such as the main form
519 of Lamin Dm_0 are targeted by stv to the CASA complex. Those proteins that cannot be
520 refolded are then tagged with poly-ubiquitin to signal their degradation through the
521 autophagosome/lysosome pathway. These poly-ubiquitinated proteins are handed off by
522 stv to ref(2)p in a process mediated by activated p38Kb. We hypothesize that this hand
523 off is a rapid process as we were unable to detect the higher molecular weight poly-
524 ubiquitinated forms binding to the CASA complex and were only able to capture these
525 transient interactions using the $p38Kb^{KD}$ construct. This model explains our finding that
526 in p38Kb mutants these poly-ubiquitinated proteins accumulate and then form
527 aggregates, and how over-expression of p38Kb would lead to increased efficiency of the
528 poly-ubiquitinated proteins being targeted to the autophagosome. In agreement with our
529 model, full-length Lamin Dm_0 would bind to the CASA complex for refolding and release,
530 or for poly-ubiquitination and transfer to ref(2)p for degradation through an interaction
531 with p38Kb.
532
533 **Discussion**
534 We find that the aging gene p38Kb regulates age-dependent protein homeostasis
535 through an interaction with the CASA complex and is acting at a step between the poly-
536 ubiquitination of an un-foldable target and its transfer to ref(2)p for autolysosomal
537 mediated degradation. Interestingly, we find that p38Kb is important for the proper
538 localization of stv to the Z-disc but does not affect the localization of other complex
539 members. This suggests that p38Kb may play a role in maintaining the interaction
540 between stv and the CASA complex which may be necessary for target transfer to

541 ref(2)p. stv has a conserved MAPK docking site as well as eight potential p38K
542 phosphorylation sites. Furthermore, the mammalian ref(2)p homolog p62 has been
543 shown in vitro to bind to mammalian p38K through two domains [74], which are partially
544 conserved in flies. Therefore, one possibility is that p38Kb mediated phosphorylation of
545 stv facilitates the localization of stv to form a functional CASA complex at the Z-disc,
546 where damaged proteins are rapidly turned over. Another possibility is that p38Kb binds
547 to stv and ref(2)p, and that the phosphorylation of stv is required for target hand-over to
548 ref(2)p so that in the absence of p38Kb, stv cannot transfer targets to ref(2)p. A
549 consequence of this may be that stv and the protein target together are released from
550 the CASA complex, leading to mislocalization of stv. As we don't detect a decrease in
551 phospho-Lamin in the p38Kb mutants or find that the p38Kb can pull-down phospho-
552 Lamin, it is unlikely that p38Kb is directly phosphorylating the target proteins as a part of
553 the stv-ref(2)p hand-over process.
554
555 How protein aggregation contributes to aging and disease has been an area of
556 great interest. One outstanding question is if protein aggregation is a consequence or
557 cause of aging. It has been hypothesized that protein aggregates accumulate with age
558 as the amount of damaged or misfolded proteins increase. However, it is not clear
559 whether or not these aggregating proteins are toxic leading to tissue dysfunction and a
560 disease state. Previous studies have found that long-lived fly strains such as over-
561 expression of Foxo or parkin result in reduced protein aggregate formation [4,75].
562 Therefore, we hypothesized that decreased protein aggregation would lead to a lifespan
563 extension, while increased protein aggregation would lead to a reduced lifespan. As
564 expected, we find that the short-lived p38Kb mutants, which exhibit premature locomotor
565 behavior defects[16], have large and numerous protein aggregates. We also find that over-
566 expression of p38Kb leads to decreased protein aggregation and increased lifespan.

However, while inhibition of stv results in increased aggregation and decreased lifespan, over-expression of stv leads to decreased aggregate number without a concurrent lifespan extension. These data suggest that protein aggregation and lifespan may be separable processes. The CASA complex is important for maintaining lifespan as inhibition of stv results in a shorter lifespan. However, as stv over-expression on its own doesn't extend lifespan, this suggests that lifespan extension may not entirely depend on the CASA complex or that increasing the activity of the CASA complex alone is not sufficient to drive lifespan. It has been hypothesized that the CASA complex is selective and only targets a subset of proteins for refolding/degradation. This selectivity is provided by BAG-3 in mammals and presumably stv in flies, though the selectivity of the complex has not been fully characterized in flies. This selectivity may explain why the CASA complex alone does not extend lifespan, as it may not target proteins that are known to cause increased lifespan but rather targets proteins that are involved in maintaining organismal health/lifespan.

Another potential interpretation of these results is that aggregate number is not as critical as aggregate size and/or content, particularly early in life, for lifespan extension. We find that stv over-expression only results in decreased aggregate size in older animals, however, co-over-expression of p38Kb and stv leads to reduced aggregate size at both young and old ages and leads to a further increase in lifespan. Thus, the turnover of specific toxic protein or subset of proteins early in life may lead to a reduction in the exposure to these toxic species and a lifespan extension. Furthermore, it has been hypothesized that protein aggregates may be protective in some instances. For example in Alzheimer's disease it has been hypothesized that the soluble form of Amyloid-β is toxic and that the formation of aggregates protects against this toxicity [76–

593 [80]. If aging or lifespan is dictated by the presence of soluble toxic proteins, then reducing
594 these toxic proteins would increase lifespan. As over-expression of stv is unable to
595 extend lifespan, this would then suggest that these particular soluble toxic proteins are
596 not targets of the CASA complex.
597
598 Our data also suggest that the p38Kb can mediate lifespan through additional,
599 CASA complex-independent mechanisms. Indeed, we have previously shown that
600 p38Kb regulates lifespan at least in part by regulating oxidative stress[16]. Additionally, we
601 find that over-expression of Hsc70-4, which is involved multiple protein quality control
602 pathways, is able to extend life span, supporting the idea that CASA alone may not be
603 sufficient to clear out all the toxic protein species that play a role in aging.
604
605 It has recently been found that over-expression of the related Hsp70 Ab gene in
606 *Drosophila* adult muscle does not extend lifespan[81]. One possibility as to why we
607 observe a lifespan extension is that we over-expressed Hsc70-4 using a different GAL4
608 driver (Mef2-GAL4 as compared to DJ694-GAL4) that drives expression all through
609 development and in the adult though expression in the adult declines with age (Figure
610 S2D). It may be that this early over-expression of Hsc70-4 provides a beneficial effect
611 that protects the fly from general life stress, resulting in increased longevity. Another
612 possibility is that Hsc70-4 and Hsp70 Ab proteins, which are 89.6% similar and 73%
613 identical, have different cellular specificities that give rise to different functions resulting
614 in different lifespan responses.
615
616 We find that Lamin, which is mutated to an aggregation prone protein form in
617 Hutchinson-Gilford progeria [46,55,57,72,82], is a target of p38Kb and the CASA complex.
618 Interestingly, p38Kb and Lamin mutants share similar phenotypes such as age-

619 dependent locomotor impairments [16,64,65] and upregulation of the Nrf-2/Keap-1 pathway
620 [16,51]. As loss of p38Kb leads to an accumulation of Lamin in the aggregates, this may be
621 toxic to the cell, leading to impaired locomotor function, increased stress and decreased
622 lifespan. Thus, we have found that one aging gene (p38Kb) regulates a second,
623 unrelated aging gene (Lamin) via the CASA complex. These data suggest a new link
624 between aging pathways and how they may converge through the regulation of protein
625 homeostasis.
626

627 **Acknowledgements**

628 We would also like to acknowledge the Bloomington Drosophila Stock Center (NIH
629 P40OD018537), the Vienna Drosophila Resource Center, and Kyoto Stock Center for
630 providing fly stocks used in this study. A. Vrailas-Mortimer was funded by start-up funds
631 from the University of Denver, a Knoebel Center for the Study of Aging pilot grant, start-
632 up funds from Illinois State University and was supported by the National Institute of
633 Arthritis and Musculoskeletal and Skin Diseases of the National Institutes of Health
634 under Award Number R15AR070505. The content is solely the responsibility of the
635 authors and does not necessarily represent the official views of the National Institutes of
636 Health. S. Sanyal was funded by startup funds from Emory University. S. Ryan was
637 supported by a Knoebel Center for the Study of Aging pilot grant to A. Vrailas-Mortimer
638 and S. Barbee, N. Mortimer was funded by start-up funds from Illinois State University.
639 The funders had no role in study design, data collection and analysis, decision to
640 publish, or preparation of the manuscript.
641
642

643 **Figure Legends**

644

645 **Fig 1. p38Kb regulates age-dependent protein homeostasis.**

646 Confocal micrographs of polyubiquitin positive protein aggregates in the adult indirect
647 flight muscle in **A)** a precise excision genetic background control p38Kb$^{Ex41/\ Ex41}$ and **B)**
648 p38Kb $^{\Delta45/\Delta45}$ null mutants at three weeks of age and in **C)** outcrossed Mef2-GAL4
649 controls (Mef2>w^{11118}) and **D)** UAS-p38Kb^{wt} Mef2-GAL4 (Mef2>p38Kb^{wt}) over-expression
650 animals at 5 weeks of age. Scale bar equals 6.2 μm. Box-Whisker plots of aggregate
651 number in p38Kb $^{\Delta45/\Delta45}$ mutants as compared to p38Kb$^{Ex41/Ex41}$ controls at **E)** 1 week and
652 **F)** 3 weeks of age and aggregate size at **G)** 1 week and **H)** 3 weeks of age. Aggregate
653 number in p38Kb^{KD} Mef2-GAL4 (Mef2>p38Kb^{KD}) and outcrossed Mef2-GAL4 controls at
654 **I)** 1 week and **J)** 5 weeks of age and aggregate size at **K)** 1 week and **L)** 5 weeks of
655 age. Aggregate number in strong p38Kb over-expression animals and outcrossed Mef2-
656 GAL4 controls at **M)** 1 week and **N)** 5 weeks of age and aggregate size at **O)** 1 week
657 and **P)** 5 weeks of age. Aggregate number in moderate p38Kb over-expression
658 (MHC>p38Kb^{wt}) animals and outcrossed MHC-GAL4 controls (MHC>w^{1118}) at **Q)** 1 week
659 and **R)** 5 weeks of age and aggregate size at **S)** 1 week and **T)** 5 weeks of age.

660

661 **Fig 2. p38Kb regulates aging phenotypes through ref(2)p.**

662 **A-C)** A subset of polyubiquitinated protein aggregates (green) in 3 week old
663 p38Kb^{Ex4}/^{Ex41} control muscle contain K63 ubiquitinated (magenta) proteins (white
664 arrows). **D-F)** K63 ubiquitin positive protein aggregates are also observed in 3 week old
665 p38Kb$^{\Delta45/\Delta45}$ mutant muscle. Protein aggregate number in ref(2)p heterozygous mutant
666 backgrounds at **G)** 1 week and **H)** 5 weeks. Loss of a single copy of ref(2)p prevents the
667 p38Kb mediated reduced protein aggregation at 1 week and 5 weeks of age. Asterisks
668 denote a p-value of ≤0.001.

669

670 **Fig 3. p38Kb genetically interacts with stv to regulate protein homeostasis and**
671 **lifespan (A-D)** Localization of a FLAG-tagged p38Kb (green in **A-D** and **A''-D''**) in the
672 adult indirect flight muscle. **A)** FLAG-tagged p38Kb localizes to the Z-disc (arrows) as
673 exhibited by colocalization with the Z-disc protein alpha-actinin (magenta, **A'** and **A''**), as
674 well as the M-line (arrowheads). **B-D)** p38Kb colocalizes with each CASA complex
675 member (magenta, **B'-D'**) at the Z-disc. Over-expression of a FLAG tagged p38Kb in the
676 muscle in **B**) an endogenous Hsc70-GFP fusion protein background, **C**) an endogenous
677 HspB8-GFP fusion protein background, and **D)** a wildtype background with endogenous
678 levels of stv. **E-F)** Muscle lysates expressing control and Mef2-GAL4 UAS-p38Kb$^{KD\text{-}FLAG}$
679 in either **E)** an endogenously expressed HspB8-GFP background or **F)** a wildtype
680 background were immunoprecipitated using anti-FLAG coated beads. **E)** Immunoblots
681 were probed with anti-GFP to detect the presence of HspB8 in the IP lysates or with **F)**
682 anti-stv to detect the presence of stv in the IP lysates. **G)** Muscle lysates expressing
683 control, UAS-mito-GFP, endogenously tagged stv or HspB8, or over-expressing MHC-
684 GAL4 UAS-Lamin^{GFP} were immunoprecipitated using anti-GFP coated beads.
685 Endogenous Lamin (~75kDa) was pulled down by stv-GFP. In addition, Lamin-GFP
686 (~100kDa) was also detected as a control. Endogenous phoshop-p38K was pulled down
687 by both stv and lamin. Endogenous stv (~80kDa) was pulled down by both HspB8 and
688 Lamin. In addition, as a control we can detect pull down of the stv-GFP (~100kDa). Anti-
689 GFP was used to confirm to the pull down of both GFP alone and HspB8-GFP.
690
691 **Fig 4. p38Kb genetically interacts with stv to regulate protein homeostasis and**
692 **lifespan. A)** Protein aggregate number and **B)** size in the moderate stv knockdown
693 background using MHC-GAL4 at 5 weeks. Asterisks denote a p-value of ≤0.001. **C)**
694 Moderate over-expression of p38Kb (red line) results in an increased lifespan as
695 compared to the MHC-GAL4 controls and p38Kb transgene control (black line and gray

696 lines, respectively). Moderate knockdown of stv using the MHC-GAL4 results in a
697 decreased lifespan (pink line compared to yellow and black lines) and is rescued by
698 p38Kb over-expression (compare pink line to blue line). **D)** Strong over-expression of
699 p38Kb (red line) results in an increased lifespan as compared to the Mef2-GAL4 controls
700 and p38Kb transgene control (black line and gray lines, respectively). Strong knockdown
701 of stv using the Mef2-GAL4 results in a decreased lifespan (pink line compared to yellow
702 and black lines) and is partially rescued by p38Kb over-expression (compare pink line to
703 blue line). **E)** Over-expression of stv in the p38Kb mutant background results in a further
704 reduction of lifespan as compared to p38Kb mutant controls (compare blue line to red
705 and grey lines).
706
707 **Fig 5. p38Kb is limiting for stv function and localization.**
708 Protein aggregate number at **A)** 1 week and **B)** 5 weeks and protein aggregate size at
709 **C)** 1 week and **D)** 5 weeks measured in stv over-expression backgrounds. Over-
710 expression of stv leads to reduced aggregate number at 1 and 5 weeks and aggregate
711 size at 5 weeks. Co-over-expression of stv and p38Kb does not result in a further
712 decrease in protein aggregate number but trends towards decreased aggregate size at
713 both 1 and 5 weeks of age. Asterisks denote a p-value of ≤0.001 when compared to the
714 GAL4 control. **E)** Over-expression of stv alone has no significant effect on lifespan (pink
715 line as compared to yellow and black lines), however, co-over-expression of stv and
716 p38Kb results in a further increase in lifespan (compare red line to blue line). **F)**
717 Immunoblots of stv from 1 and 3 week old muscle lysates of control and p38Kb mutants.
718 **G)** stv localizes to the adult muscle Z-disc and M-line (white arrows) in control animals.
719 **H)** stv localization is disrupted in p38Kb mutants. **I)** Quantification of average pixel
720 density.
721

722 **Fig 6. p38Kb and stv regulate Lamin aggregation.**

723 **A)** Immunoblot analysis of stv-RNAi and GAL4 controls flies muscle lysates probed with
724 anti-Lamin and **B)** quantified using densitometry, asterisk denotes p value=0.028. **C)**
725 Immunoblot analysis of p38Kb$^{Ex41/Ex41}$ control and p38Kb $^{\Delta45/\Delta45}$ mutant muscle lysates
726 probed with anti-Lamin and **D)** quantified using densitometry, asterisk denotes p value =
727 0.006643. **E)** Immunoblot analysis of p38Kb$^{Ex41/Ex41}$ control and p38Kb $^{\Delta45/\Delta45}$ mutant
728 muscle lysates probed with anti-phospho Lamin and **F)** quantified using densitometry,
729 p=0.09. **G)** p38Kb^{KD} was expressed in muscles using Mef2-GAL4. p38Kb was
730 immunoprecipitated from adult muscle lysates using anti-FLAG coated beads.
731 Immunoblots were probed with anti-lamin and anti-FLAG.

732

733 **Fig 7. Lamin aggregation is increased in aged p38Kb mutants.**

734 **A-C)** Immunoblots of sucrose gradient fractions from 3 week old p38Kb$^{Ex41/Ex41}$ control
735 and p38Kb $^{\Delta45/\Delta45}$ mutant muscle. **A)** The main species of Lamin (~75kDa) is mainly
736 found in fractions 5-7 with some in the pellet, and the farnesylated form of Lamin
737 (~100kDa) is mostly found in the pellet in controls. In the p38Kb mutants, there is a
738 further accumulation of Lamin and farnesylated Lamin in the pellet. **B)** Phosphorylated
739 Lamin is also found predominantly in fractions 5-7 in controls and accumulates in the
740 pellet in p38Kb mutants. **C)** Poly-ubiquitin is found mostly in the pellet fraction, marking
741 the protein aggregates. **D)** Immunoblots of control and Lamin^{A25} mutants that lack the
742 CAAX motif demonstrate the loss of the farnesylated form of Lamin (100kDa) without
743 affecting the main form of Lamin (~75kDa). In addition, phosphorylated Lamin is also
744 present in the Lamin mutants.

745

746

747

748

749 **References**

750 1. Taylor, R. C. & Dillin, A. Aging as an event of proteostasis collapse. *Cold Spring*
751 *Harb. Perspect. Biol.* **3**, (2011).
752 2. Ben-Zvi, A., Miller, E. A. & Morimoto, R. I. Collapse of proteostasis represents an
753 early molecular event in Caenorhabditis elegans aging. *Proc. Natl. Acad. Sci. U. S.*
754 *A.* **106**, 14914–14919 (2009).
755 3. Cohen, E., Bieschke, J., Perciavalle, R. M., Kelly, J. W. & Dillin, A. Opposing
756 activities protect against age-onset proteotoxicity. *Science* **313**, 1604–1610 (2006).
757 4. Demontis, F. & Perrimon, N. FOXO/4E-BP signaling in Drosophila muscles regulates
758 organism-wide proteostasis during aging. *Cell* **143**, 813–825 (2010).
759 5. Morley, J. F., Brignull, H. R., Weyers, J. J. & Morimoto, R. I. The threshold for
760 polyglutamine-expansion protein aggregation and cellular toxicity is dynamic and
761 influenced by aging in Caenorhabditis elegans. *Proc. Natl. Acad. Sci. U. S. A.* **99**,
762 10417–10422 (2002).
763 6. Palazzolo, I. *et al.* Overexpression of IGF-1 in muscle attenuates disease in a mouse
764 model of spinal and bulbar muscular atrophy. *Neuron* **63**, 316–328 (2009).
765 7. Schnöder, L. *et al.* Deficiency of Neuronal p38α MAPK Attenuates Amyloid
766 Pathology in Alzheimer Disease Mouse and Cell Models through Facilitating
767 Lysosomal Degradation of BACE1. *J. Biol. Chem.* **291**, 2067–2079 (2016).
768 8. Webber, J. L. & Tooze, S. A. New insights into the function of Atg9. *FEBS Lett.* **584**,
769 1319–1326 (2010).
770 9. Liu, B., Cheng, Y., Zhang, B., Bian, H. & Bao, J. Polygonatum cyrtonema lectin
771 induces apoptosis and autophagy in human melanoma A375 cells through a
772 mitochondria-mediated ROS-p38-p53 pathway. *Cancer Lett.* **275**, 54–60 (2009).

773 10. Younce, C. W. & Kolattukudy, P. E. MCP-1 causes cardiomyoblast death via
774 autophagy resulting from ER stress caused by oxidative stress generated by
775 inducing a novel zinc-finger protein, MCPIP. *Biochem. J.* **426**, 43–53 (2010).
776 11. Duan, W.-J. *et al.* Silibinin activated p53 and induced autophagic death in human
777 fibrosarcoma HT1080 cells via reactive oxygen species-p38 and c-Jun N-terminal
778 kinase pathways. *Biol. Pharm. Bull.* **34**, 47–53 (2011).
779 12. Zhuang, Y., Li, Y., Li, X., Xie, Q. & Wu, M. Atg7 Knockdown Augments Concanavalin
780 A-Induced Acute Hepatitis through an ROS-Mediated p38/MAPK Pathway. *PloS One*
781 **11**, e0149754 (2016).
782 13. Henson, S. M. *et al.* p38 signaling inhibits mTORC1-independent autophagy in
783 senescent human $CD8^+$ T cells. *J. Clin. Invest.* **124**, 4004–4016 (2014).
784 14. Luo, Y. *et al.* Autophagy regulates ROS-induced cellular senescence via p21 in a
785 p38 MAPKα dependent manner. *Exp. Gerontol.* **46**, 860–867 (2011).
786 15. Rudolf, E., Rezáčová, K. & Cervinka, M. Activation of p38 and changes in
787 mitochondria accompany autophagy to premature senescence-like phenotype switch
788 upon chronic exposure to selenite in colon fibroblasts. *Toxicol. Lett.* **231**, 29–37
789 (2014).
790 16. Vrailas-Mortimer, A. *et al.* A muscle-specific p38 MAPK/Mef2/MnSOD pathway
791 regulates stress, motor function, and life span in Drosophila. *Dev. Cell* **21**, 783–795
792 (2011).
793 17. Belozerov, V. E., Ratkovic, S., McNeill, H., Hilliker, A. J. & McDermott, J. C. In vivo
794 interaction proteomics reveal a novel p38 mitogen-activated protein kinase/Rack1
795 pathway regulating proteostasis in Drosophila muscle. *Mol. Cell. Biol.* **34**, 474–484
796 (2014).
797 18. Guruharsha, K. G. *et al.* A protein complex network of Drosophila melanogaster. *Cell*
798 **147**, 690–703 (2011).

799 19. Arndt, V. *et al.* Chaperone-assisted selective autophagy is essential for muscle
800 maintenance. *Curr. Biol. CB* **20**, 143–148 (2010).
801 20. Stürner, E. & Behl, C. The Role of the Multifunctional BAG3 Protein in Cellular
802 Protein Quality Control and in Disease. *Front. Mol. Neurosci.* **10**, 177 (2017).
803 21. Behl, C. BAG3 and friends: co-chaperones in selective autophagy during aging and
804 disease. *Autophagy* **7**, 795–798 (2011).
805 22. Gamerdinger, M. *et al.* Protein quality control during aging involves recruitment of
806 the macroautophagy pathway by BAG3. *EMBO J.* **28**, 889–901 (2009).
807 23. Kettern, N., Dreiseidler, M., Tawo, R. & Höhfeld, J. Chaperone-assisted degradation:
808 multiple paths to destruction. *Biol. Chem.* **391**, 481–489 (2010).
809 24. Min, J.-N. *et al.* CHIP deficiency decreases longevity, with accelerated aging
810 phenotypes accompanied by altered protein quality control. *Mol. Cell. Biol.* **28**, 4018–
811 4025 (2008).
812 25. Terman, A., Gustafsson, B. & Brunk, U. T. Autophagy, organelles and ageing. *J.*
813 *Pathol.* **211**, 134–143 (2007).
814 26. Dietzl, G. *et al.* A genome-wide transgenic RNAi library for conditional gene
815 inactivation in Drosophila. *Nature* **448**, 151–156 (2007).
816 27. R. C. Team. R Foundation for Statistical Computing. (2015).
817 28. Lim, K. L. *et al.* Parkin mediates nonclassical, proteasomal-independent
818 ubiquitination of synphilin-1: implications for Lewy body formation. *J. Neurosci. Off.*
819 *J. Soc. Neurosci.* **25**, 2002–2009 (2005).
820 29. Olzmann, J. A. *et al.* Parkin-mediated K63-linked polyubiquitination targets misfolded
821 DJ-1 to aggresomes via binding to HDAC6. *J. Cell Biol.* **178**, 1025–1038 (2007).
822 30. Yung, C., Sha, D., Li, L. & Chin, L.-S. Parkin Protects Against Misfolded SOD1
823 Toxicity by Promoting Its Aggresome Formation and Autophagic Clearance. *Mol.*
824 *Neurobiol.* **53**, 6270–6287 (2016).

825 31. Hao, R. *et al.* Proteasomes activate aggresome disassembly and clearance by
826 producing unanchored ubiquitin chains. *Mol. Cell* **51**, 819–828 (2013).
827 32. Tan, J. M. M. *et al.* Lysine 63-linked ubiquitination promotes the formation and
828 autophagic clearance of protein inclusions associated with neurodegenerative
829 diseases. *Hum. Mol. Genet.* **17**, 431–439 (2008).
830 33. Katsuragi, Y., Ichimura, Y. & Komatsu, M. p62/SQSTM1 functions as a signaling hub
831 and an autophagy adaptor. *FEBS J.* **282**, 4672–4678 (2015).
832 34. Ulbricht, A. *et al.* Cellular mechanotransduction relies on tension-induced and
833 chaperone-assisted autophagy. *Curr. Biol. CB* **23**, 430–435 (2013).
834 35. Chakraborty, D. *et al.* Enhanced autophagic-lysosomal activity and increased BAG3-
835 mediated selective macroautophagy as adaptive response of neuronal cells to
836 chronic oxidative stress. *Redox Biol.* **24**, 101181 (2019).
837 36. Hattori, A., Mizuno, T., Akamatsu, M., Hisamoto, N. & Matsumoto, K. The
838 Caenorhabditis elegans JNK Signaling Pathway Activates Expression of Stress
839 Response Genes by Derepressing the Fos/HDAC Repressor Complex. *PLOS*
840 *Genet.* **9**, e1003315 (2013).
841 37. Ryan, S. M. *et al.* Evolutionarily Conserved Transcription Factors Drive the Oxidative
842 Stress Response in Drosophila. *bioRxiv* 735126 (2019) doi:10.1101/735126.
843 38. Coulson, M., Robert, S. & Saint, R. Drosophila starvin encodes a tissue-specific
844 BAG-domain protein required for larval food uptake. *Genetics* **171**, 1799–1812
845 (2005).
846 39. Sato, T. *et al.* DNAJB6 myopathy in an Asian cohort and cytoplasmic/nuclear
847 inclusions. *Neuromuscul. Disord. NMD* **23**, 269–276 (2013).
848 40. Selcen, D. *et al.* Mutation in BAG3 causes severe dominant childhood muscular
849 dystrophy. *Ann. Neurol.* **65**, 83–89 (2009).

850 41. Sarparanta, J. *et al.* Mutations affecting the cytoplasmic functions of the co-
851 chaperone DNAJB6 cause limb-girdle muscular dystrophy. *Nat. Genet.* **44**, 450–455,
852 S1-2 (2012).
853 42. Fanzani, A. *et al.* Hypertrophy and atrophy inversely regulate Caveolin-3 expression
854 in myoblasts. *Biochem. Biophys. Res. Commun.* **357**, 314–318 (2007).
855 43. Capanni, C. *et al.* Dysferlin in a hyperCKaemic patient with caveolin 3 mutation and
856 in C2C12 cells after p38 MAP kinase inhibition. *Exp. Mol. Med.* **35**, 538–544 (2003).
857 44. Suzuki, N. *et al.* Continuous administration of poloxamer 188 reduces overload-
858 induced muscular atrophy in dysferlin-deficient SJL mice. *Neurosci. Res.* **72**, 181–
859 186 (2012).
860 45. De Sandre-Giovannoli, A. *et al.* Lamin a truncation in Hutchinson-Gilford progeria.
861 *Science* **300**, 2055 (2003).
862 46. Eriksson, M. *et al.* Recurrent de novo point mutations in lamin A cause Hutchinson-
863 Gilford progeria syndrome. *Nature* **423**, 293–298 (2003).
864 47. Mounkes, L. C., Kozlov, S., Hernandez, L., Sullivan, T. & Stewart, C. L. A progeroid
865 syndrome in mice is caused by defects in A-type lamins. *Nature* **423**, 298–301
866 (2003).
867 48. Singla, A. *et al.* Lamin aggregation is an early sensor of porphyria-induced liver
868 injury. *J. Cell Sci.* **126**, 3105–3112 (2013).
869 49. Bank, E. M. *et al.* A laminopathic mutation disrupting lamin filament assembly
870 causes disease-like phenotypes in Caenorhabditis elegans. *Mol. Biol. Cell* **22**, 2716–
871 2728 (2011).
872 50. Casasola, A. *et al.* Prelamin A processing, accumulation and distribution in normal
873 cells and laminopathy disorders. *Nucleus* **7**, 84–102 (2016).
874 51. Dialynas, G. *et al.* Myopathic Lamin Mutations Cause Reductive Stress and Activate
875 the Nrf2/Keap-1 Pathway. *PLOS Genet.* **11**, e1005231 (2015).

876 52. Hübner, S., Eam, J. E., Hübner, A. & Jans, D. A. Laminopathy-inducing lamin A
877 mutants can induce redistribution of lamin binding proteins into nuclear aggregates.
878 *Exp. Cell Res.* **312**, 171–183 (2006).
879 53. Hübner, S., Eam, J. E., Wagstaff, K. M. & Jans, D. A. Quantitative analysis of
880 localization and nuclear aggregate formation induced by GFP-lamin A mutant
881 proteins in living HeLa cells. *J. Cell. Biochem.* **98**, 810–826 (2006).
882 54. Ahmed, M. S., Ikram, S., Bibi, N. & Mir, A. Hutchinson-Gilford Progeria Syndrome: A
883 Premature Aging Disease. *Mol. Neurobiol.* **55**, 4417–4427 (2018).
884 55. Barascu, A. *et al.* Oxidative stress induces an ATM-independent senescence
885 pathway through p38 MAPK-mediated lamin B1 accumulation. *EMBO J.* **31**, 1080–
886 1094 (2012).
887 56. Zaremba-Czogalla, M. *et al.* The Different Function of Single Phosphorylation Sites
888 of Drosophila melanogaster Lamin Dm and Lamin C. *PLoS ONE* **7**, (2012).
889 57. Chandran, S. *et al.* Suppression of myopathic lamin mutations by muscle-specific
890 activation of AMPK and modulation of downstream signaling. *Hum. Mol. Genet.* **28**,
891 351–371 (2019).
892 58. Smith, D. E., Gruenbaum, Y., Berrios, M. & Fisher, P. A. Biosynthesis and
893 interconversion of Drosophila nuclear lamin isoforms during normal growth and in
894 response to heat shock. *J. Cell Biol.* **105**, 771–790 (1987).
895 59. Zaremba-Czogalla, M. *et al.* Identification of new in vivo phosphosites on lamin Dm -
896 the evidence of heterogeneity of phosphorylation sites in different Drosophila
897 tissues. *Nucl. Austin Tex* **2**, 478–488 (2011).
898 60. Rzepecki, R. & Fisher, P. A. In vivo phosphorylation of Drosophila melanogaster
899 nuclear lamins during both interphase and mitosis. *Cell. Mol. Biol. Lett.* **7**, 859–876
900 (2002).

901 61. Schneider, U., Mini, T., Jenö, P., Fisher, P. A. & Stuurman, N. Phosphorylation of the
902 major Drosophila lamin in vivo: site identification during both M-phase (meiosis) and
903 interphase by electrospray ionization tandem mass spectrometry. *Biochemistry* **38**,
904 4620–4632 (1999).
905 62. Brandt, A., Krohne, G. & Grosshans, J. The farnesylated nuclear proteins
906 KUGELKERN and LAMIN B promote aging-like phenotypes in Drosophila flies.
907 *Aging Cell* **7**, 541–551 (2008).
908 63. Polychronidou, M., Hellwig, A. & Grosshans, J. Farnesylated nuclear proteins
909 Kugelkern and lamin Dm0 affect nuclear morphology by directly interacting with the
910 nuclear membrane. *Mol. Biol. Cell* **21**, 3409–3420 (2010).
911 64. Li, Y. *et al.* Lamin Mutations Accelerate Aging via Defective Export of Mitochondrial
912 mRNAs through Nuclear Envelope Budding. *Curr. Biol. CB* **26**, 2052–2059 (2016).
913 65. Muñoz-Alarcón, A. *et al.* Characterization of lamin Mutation Phenotypes in
914 Drosophila and Comparison to Human Laminopathies. *PLOS ONE* **2**, e532 (2007).
915 66. Dialynas, G., Speese, S., Budnik, V., Geyer, P. K. & Wallrath, L. L. The role of
916 Drosophila Lamin C in muscle function and gene expression. *Dev. Camb. Engl.* **137**,
917 3067–3077 (2010).
918 67. Gupta, M. K. *et al.* Lamin B is a target for selective nuclear PQC by BAG3:
919 implication for nuclear envelopathies. *Cell Death Dis.* **10**, 23 (2019).
920 68. Kitten, G. T. & Nigg, E. A. The CaaX motif is required for isoprenylation, carboxyl
921 methylation, and nuclear membrane association of lamin B2. *J. Cell Biol.* **113**, 13–23
922 (1991).
923 69. Holtz, D., Tanaka, R. A., Hartwig, J. & McKeon, F. The CaaX motif of lamin A
924 functions in conjunction with the nuclear localization signal to target assembly to the
925 nuclear envelope. *Cell* **59**, 969–977 (1989).

926 70. Meshorer, E. & Gruenbaum, Y. Gone with the Wnt/Notch: stem cells in
927 laminopathies, progeria, and aging. *J. Cell Biol.* **181**, 9–13 (2008).
928 71. Patterson, K. *et al.* The functions of Klarsicht and nuclear lamin in developmentally
929 regulated nuclear migrations of photoreceptor cells in the Drosophila eye. *Mol. Biol.*
930 *Cell* **15**, 600–610 (2004).
931 72. Cao, K., Capell, B. C., Erdos, M. R., Djabali, K. & Collins, F. S. A lamin A protein
932 isoform overexpressed in Hutchinson-Gilford progeria syndrome interferes with
933 mitosis in progeria and normal cells. *Proc. Natl. Acad. Sci. U. S. A.* **104**, 4949–4954
934 (2007).
935 73. Machowska, M., Piekarowicz, K. & Rzepecki, R. Regulation of lamin properties and
936 functions: does phosphorylation do it all? *Open Biol.* **5**, (2015).
937 74. Saito, A., Kawai, K., Takayama, H., Sudo, T. & Osada, H. Improvement of
938 photoaffinity SPR imaging platform and determination of the binding site of
939 p62/SQSTM1 to p38 MAP kinase. *Chem. Asian J.* **3**, 1607–1612 (2008).
940 75. Rana, A., Rera, M. & Walker, D. W. Parkin overexpression during aging reduces
941 proteotoxicity, alters mitochondrial dynamics, and extends lifespan. *Proc. Natl. Acad.*
942 *Sci. U. S. A.* **110**, 8638–8643 (2013).
943 76. Hayden, E. Y. & Teplow, D. B. Amyloid β-protein oligomers and Alzheimer's disease.
944 *Alzheimers Res. Ther.* **5**, 60 (2013).
945 77. Lesné, S. *et al.* A specific amyloid-β protein assembly in the brain impairs memory.
946 *Nature* **440**, 352–357 (2006).
947 78. Walsh, D. M. *et al.* Naturally secreted oligomers of amyloid β protein potently inhibit
948 hippocampal long-term potentiation in vivo. *Nature* **416**, 535–539 (2002).
949 79. Kayed, R. *et al.* Common Structure of Soluble Amyloid Oligomers Implies Common
950 Mechanism of Pathogenesis. *Science* **300**, 486–489 (2003).

951 80. Horváth, D., Menyhárd, D. K. & Perczel, A. Protein Aggregation in a Nutshell: The
952 Splendid Molecular Architecture of the Dreaded Amyloid Fibrils. *Curr. Protein Pept.*
953 *Sci.* **20**, 1077–1088 (2019).
954 81. Xiao, C. *et al.* Expression of Heat Shock Protein 70 Is Insufficient To Extend
955 Drosophila melanogaster Longevity. *G3 Bethesda Md* **9**, 4197–4207 (2019).
956 82. Burke, B. & Stewart, C. L. The nuclear lamins: flexibility in function. *Nat. Rev. Mol.*
957 *Cell Biol.* **14**, 13–24 (2013).
958

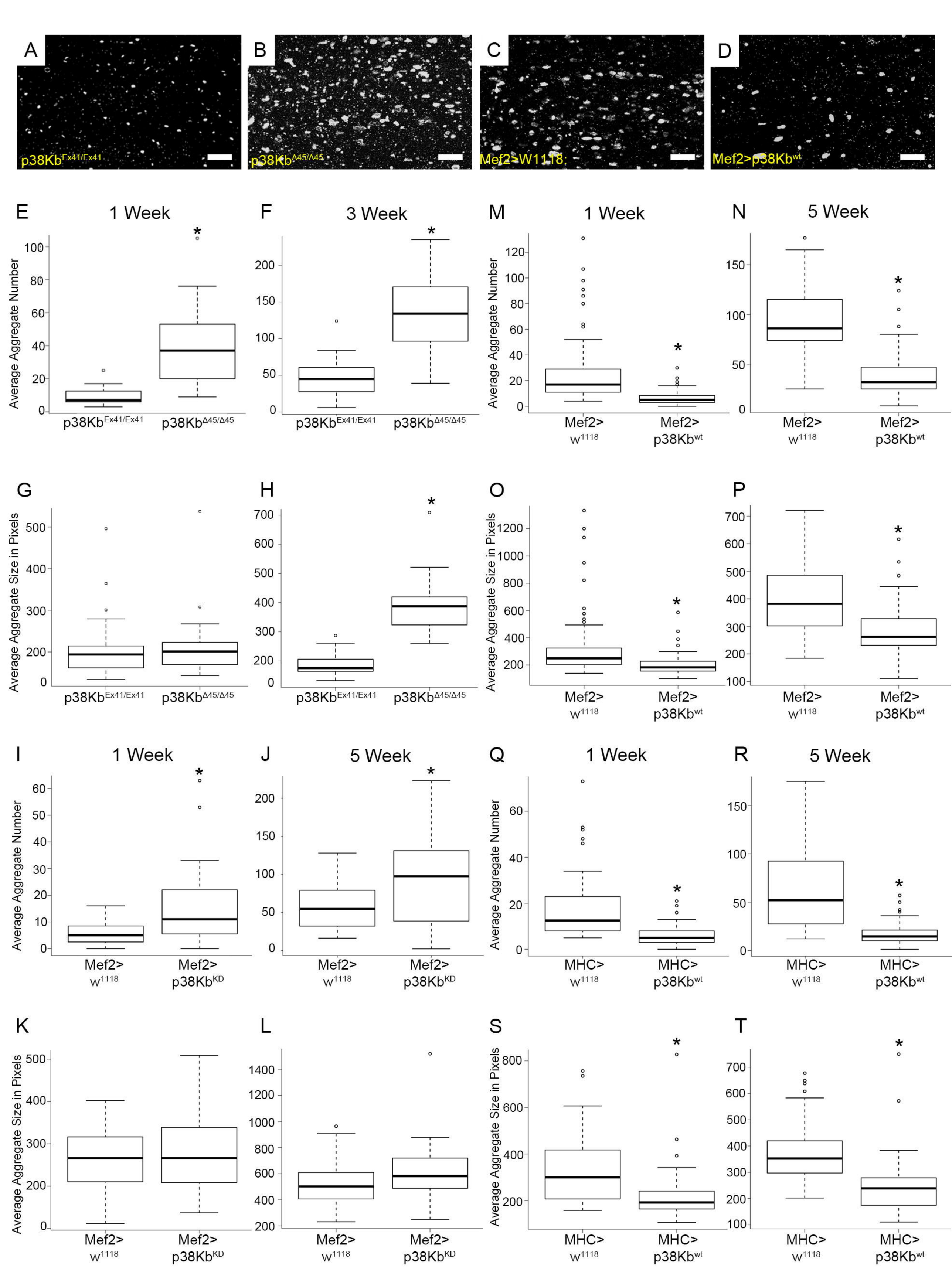
A
p38Kb Ex41/Ex41
B
p38Kb Δ45/Δ45
C
Mef2>W1118;
D
Mef2>p38Kb wt
E
1 Week
Average Aggregate Number
p38Kb Ex41/Ex41
p38Kb Δ45/Δ45
F
3 Week
M
1 Week
Average Aggregate Number
Mef2> w1118
Mef2> p38Kb wt
N
5 Week
G
Average Aggregate Size in Pixels
H
O
Average Aggregate Size in Pixels
P
I
1 Week
Average Aggregate Number
Mef2> w1118
Mef2> p38Kb KD
J
5 Week
Q
1 Week
MHC> w1118
MHC> p38Kb wt
R
5 Week
K
Average Aggregate Size in Pixels
L
S
Average Aggregate Size in Pixels
T

Figure 1

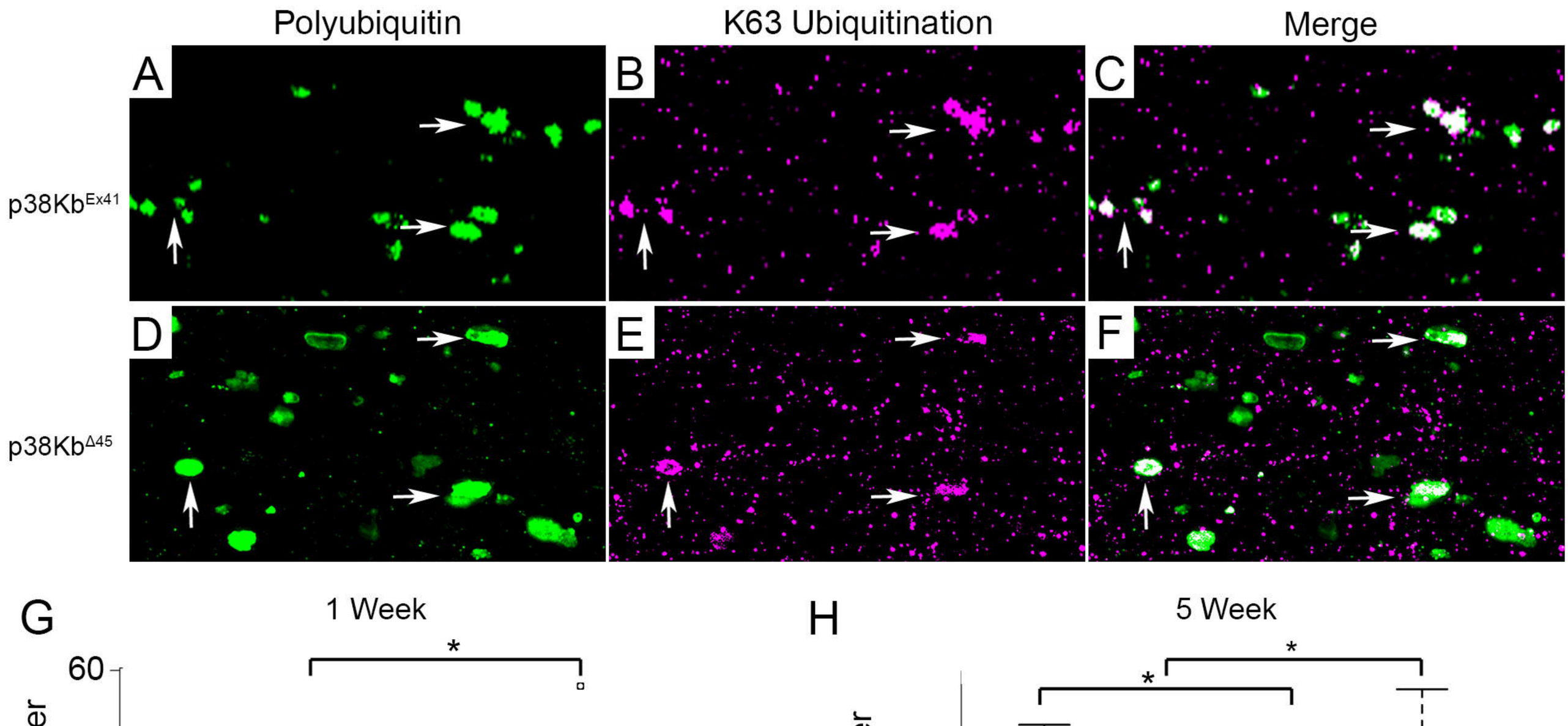
Polyubiquitin
K63 Ubiquitination
Merge
A
B
C
D
E
F
p38Kb^Ex41
p38Kb^Δ45

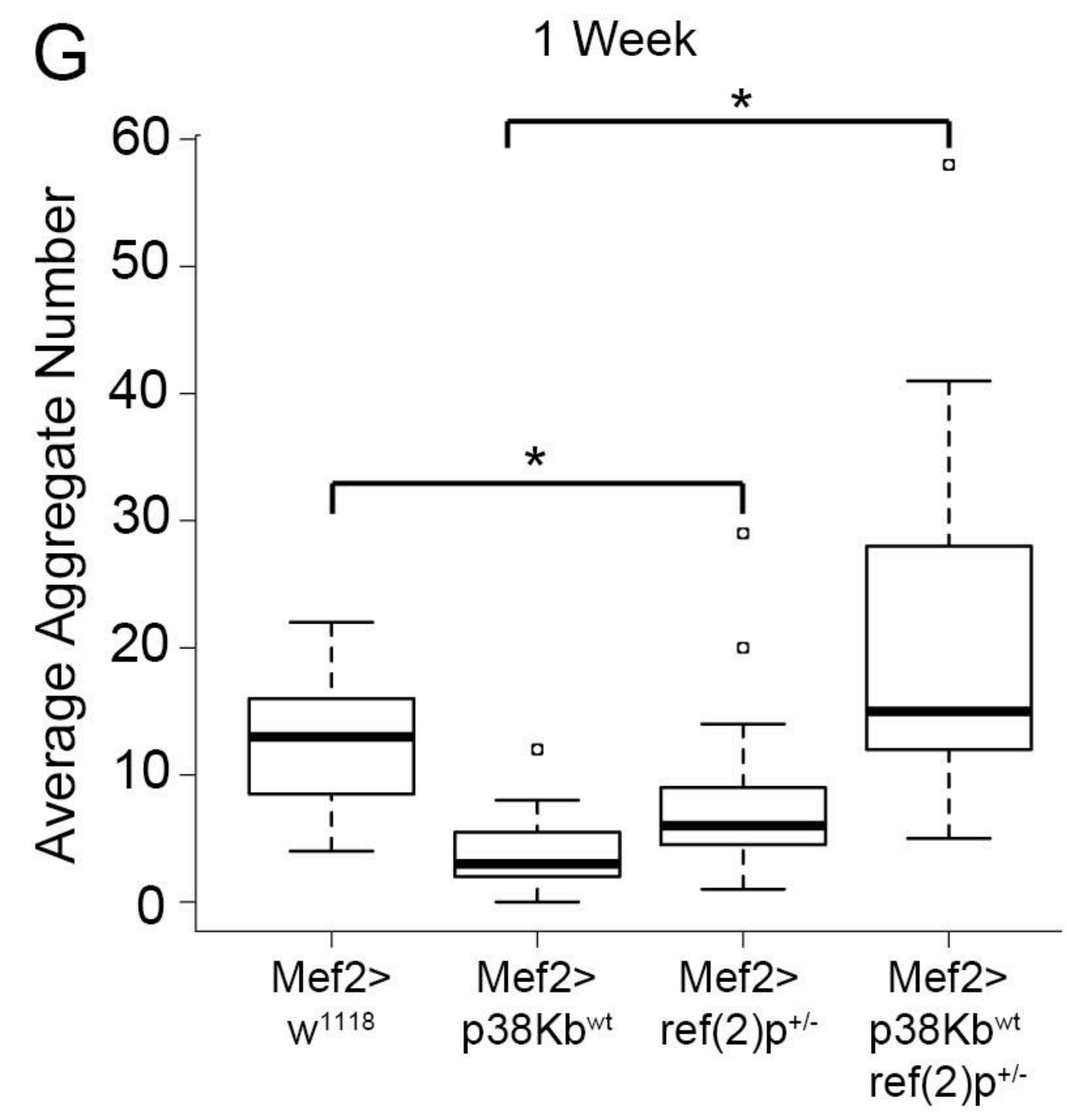
G
1 Week
Average Aggregate Number
60
50
40
30
20
10
0
*
*
Mef2> w1118
Mef2> p38Kbwt
Mef2> ref(2)p+/-
Mef2> p38Kbwt ref(2)p+/-

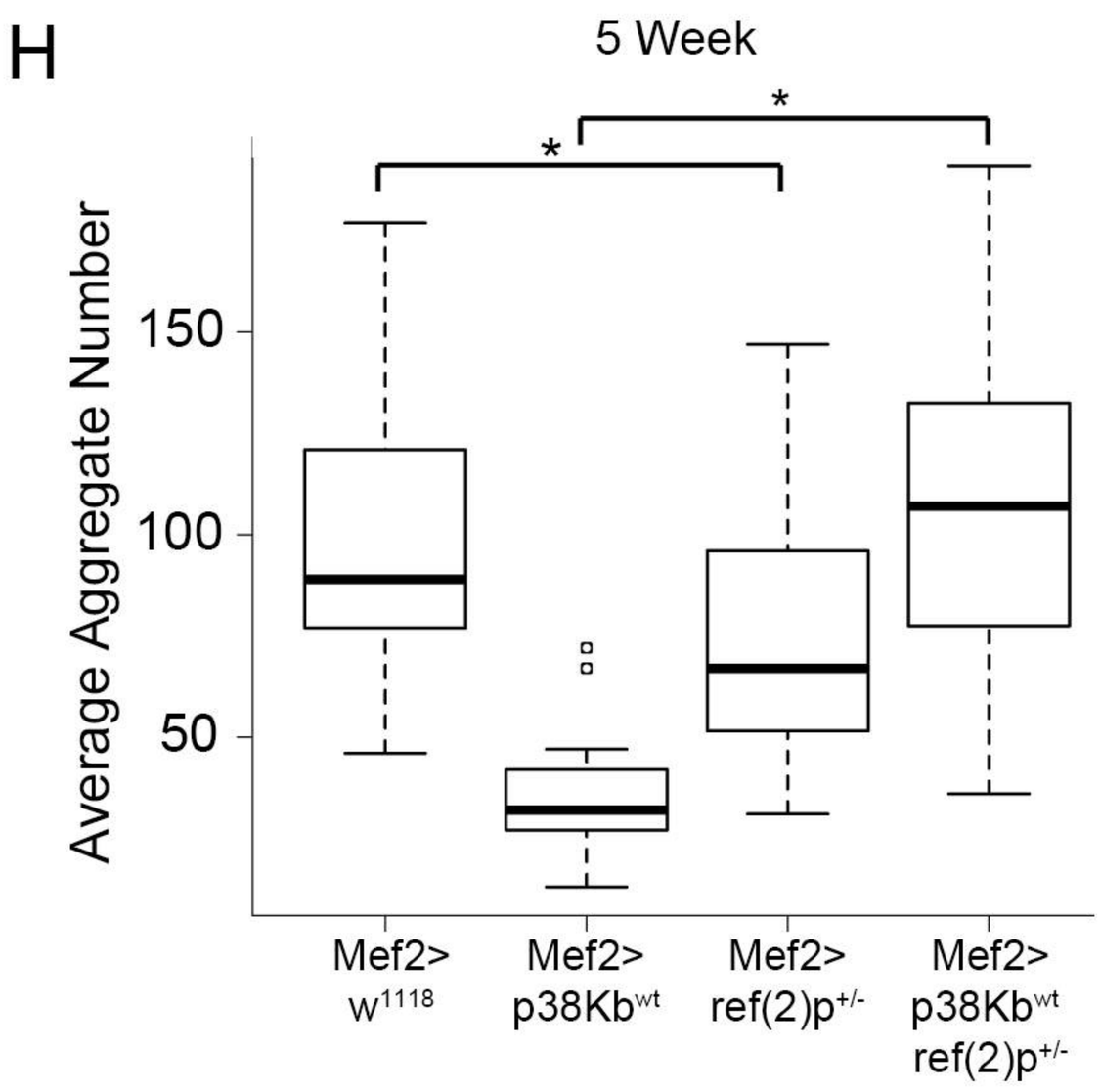
H
5 Week
Average Aggregate Number
150
100
50
*
*
Mef2> w1118
Mef2> p38Kbwt
Mef2> ref(2)p+/-
Mef2> p38Kbwt ref(2)p+/-

Figure 2

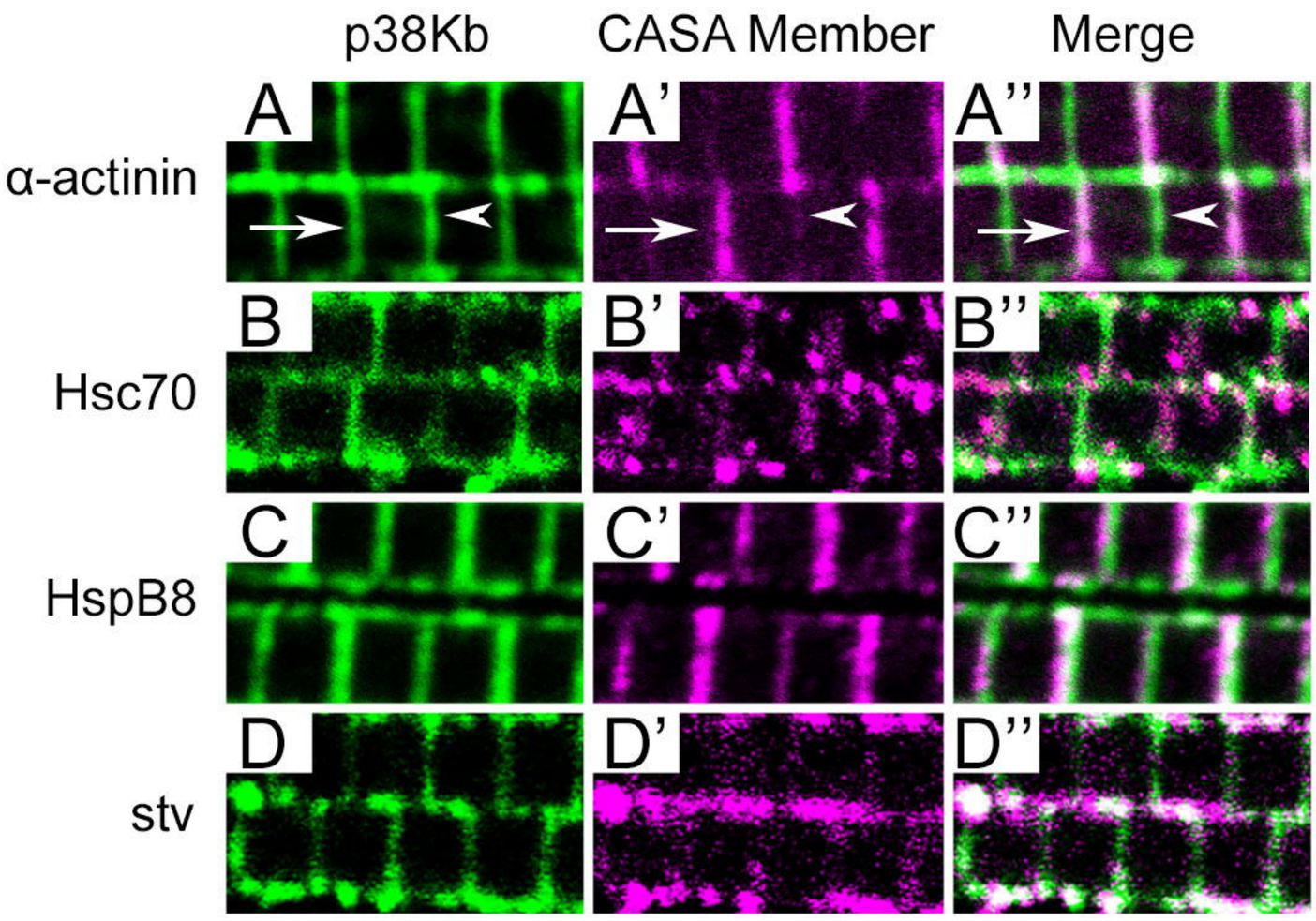
p38Kb
CASA Member
Merge
A
A'
A''
α-actinin
B
B'
B''
Hsc70
C
C'
C''
HspB8
D
D'
D''
stv

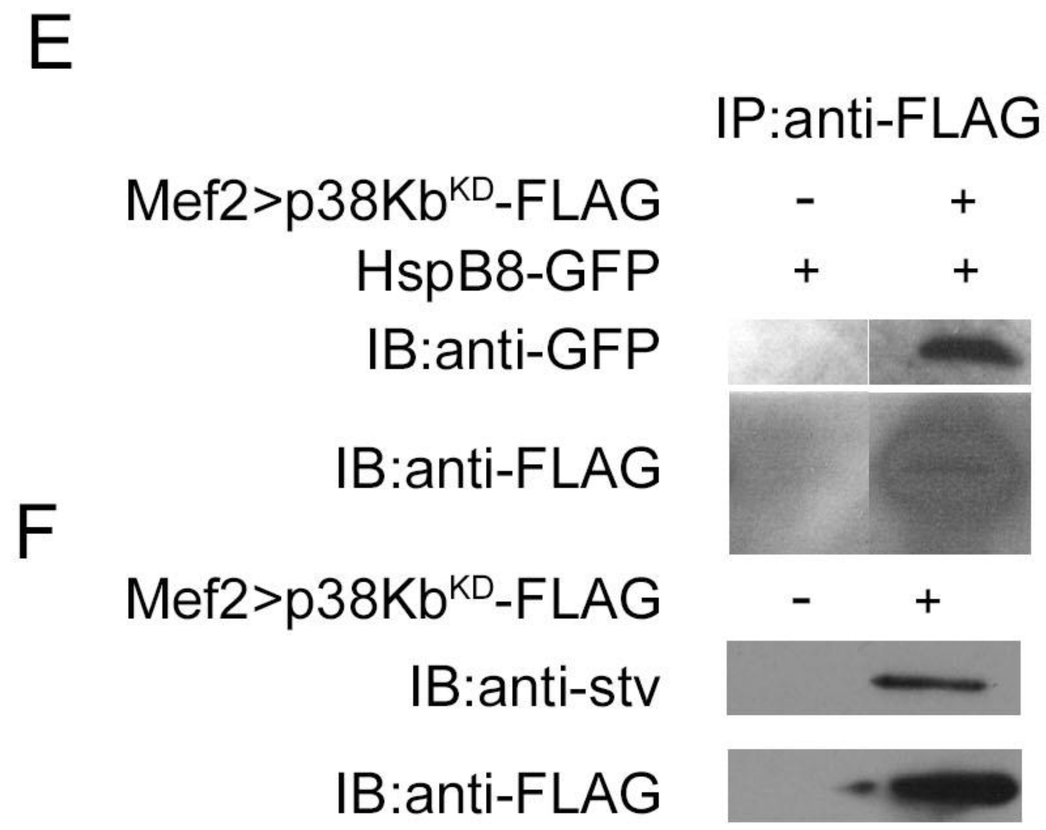
E
IP:anti-FLAG
Mef2>p38Kb^KD-FLAG - +
HspB8-GFP + +
IB:anti-GFP
IB:anti-FLAG
F
Mef2>p38Kb^KD-FLAG - +
IB:anti-stv
IB:anti-FLAG

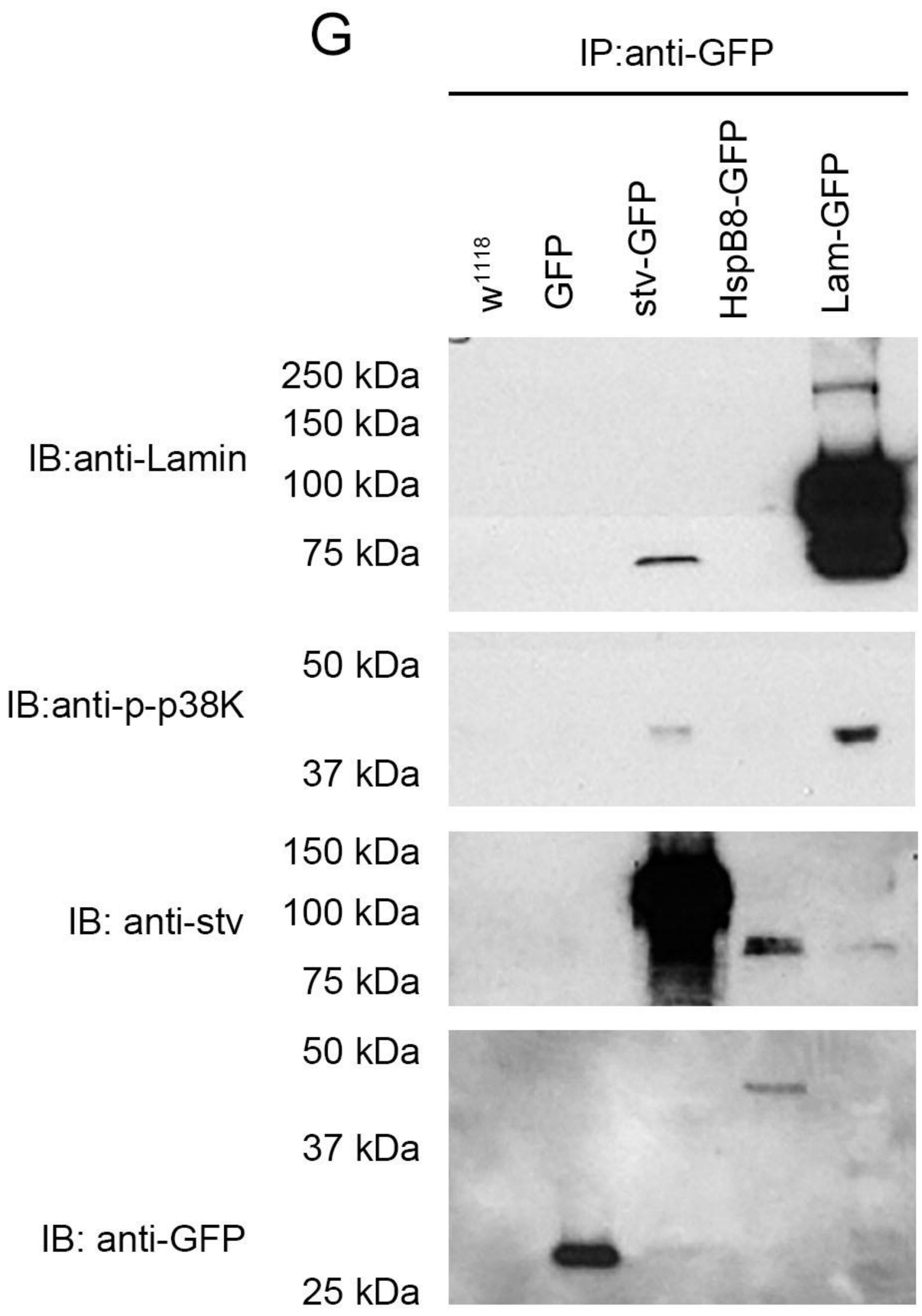
G
IP:anti-GFP
w1118
GFP
stv-GFP
HspB8-GFP
Lam-GFP
IB:anti-Lamin
250 kDa
150 kDa
100 kDa
75 kDa
IB:anti-p-p38K
50 kDa
37 kDa
IB: anti-stv
150 kDa
100 kDa
75 kDa
IB: anti-GFP
50 kDa
37 kDa
25 kDa

Figure 3

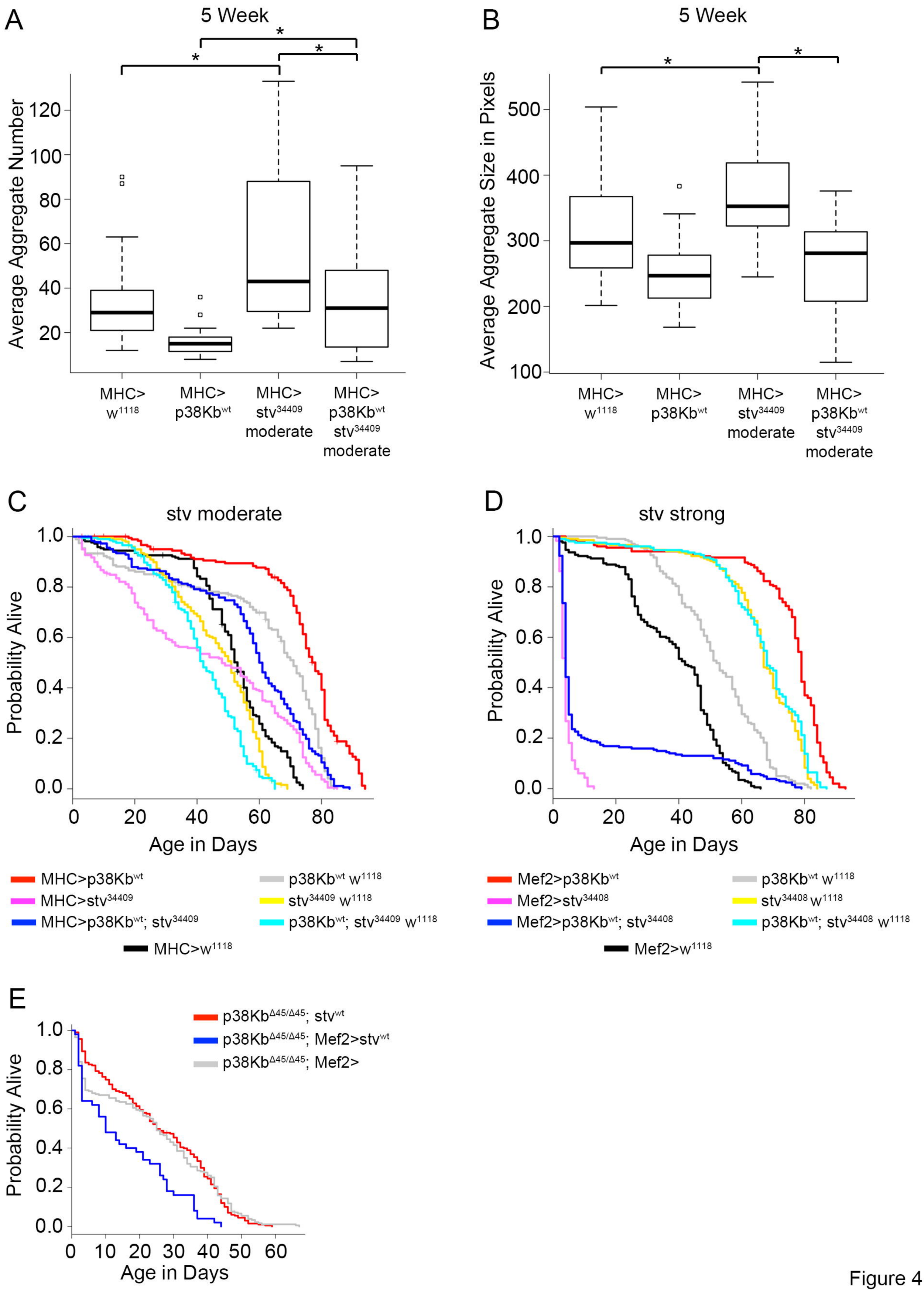
A
5 Week
Average Aggregate Number
MHC> w1118
MHC> p38Kbwt
MHC> stv34409 moderate
MHC> p38Kbwt stv34409 moderate
B
5 Week
Average Aggregate Size in Pixels
C
stv moderate
Probability Alive
Age in Days
MHC>p38Kbwt
MHC>stv34409
MHC>p38Kbwt; stv34409
MHC>w1118
p38Kbwt w1118
stv34409 w1118
p38Kbwt; stv34409 w1118
D
stv strong
Mef2>p38Kbwt
Mef2>stv34408
Mef2>p38Kbwt; stv34408
Mef2>w1118
p38Kbwt w1118
stv34408 w1118
p38Kbwt; stv34408 w1118
E
p38KbΔ45/Δ45; stvwt
p38KbΔ45/Δ45; Mef2>stvwt
p38KbΔ45/Δ45; Mef2>

Figure 4

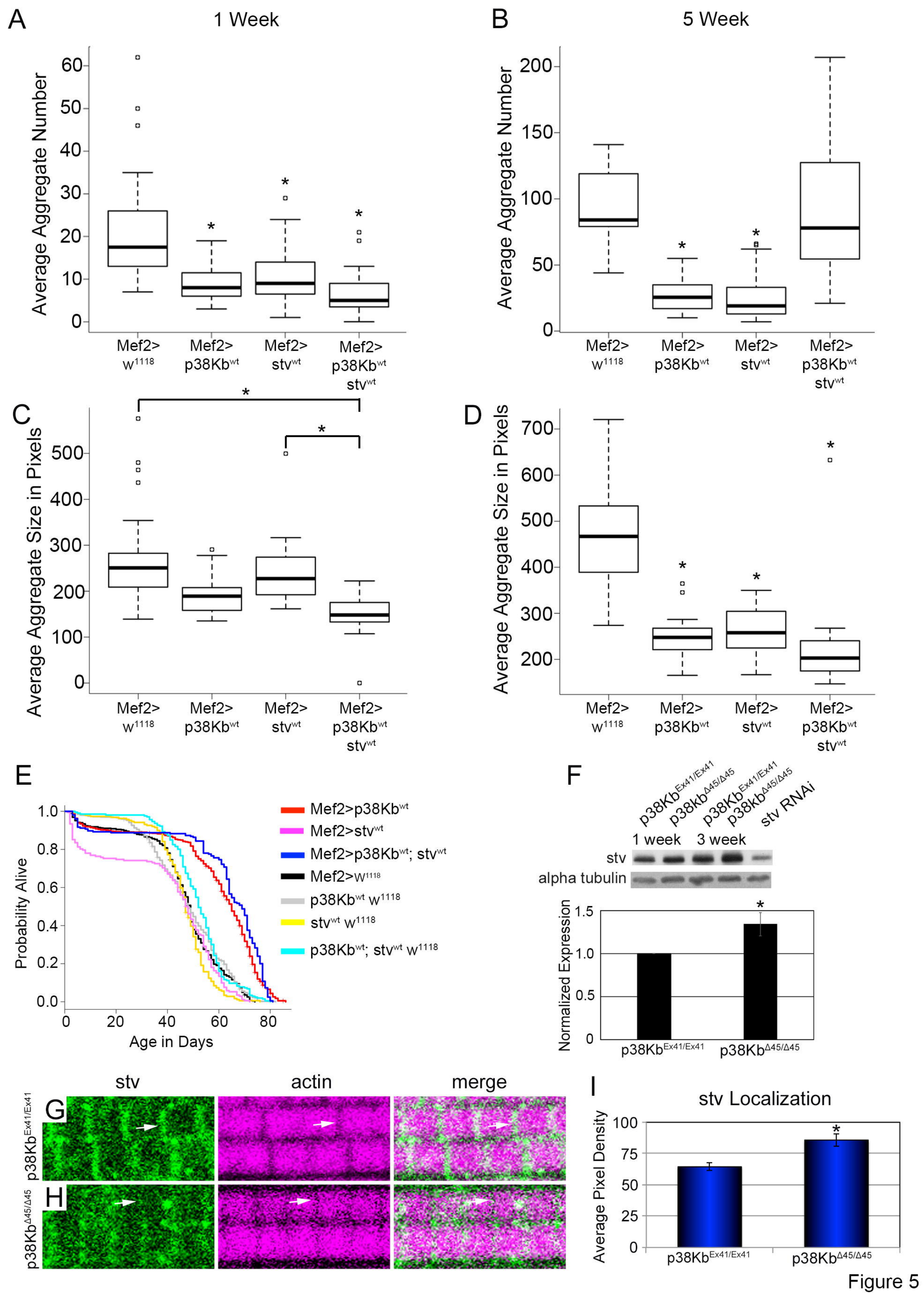
A
1 Week
Average Aggregate Number
Mef2> w1118
Mef2> p38Kbwt
Mef2> stvwt
Mef2> p38Kbwt stvwt
B
5 Week
Average Aggregate Number
C
Average Aggregate Size in Pixels
D
Average Aggregate Size in Pixels
E
Probability Alive
Age in Days
Mef2>p38Kbwt
Mef2>stvwt
Mef2>p38Kbwt; stvwt
Mef2>w1118
p38Kbwt w1118
stvwt w1118
p38Kbwt; stvwt w1118
F
p38KbEx41/Ex41
p38KbΔ45/Δ45
p38KbEx41/Ex41
p38KbΔ45/Δ45
stv RNAi
1 week
3 week
stv
alpha tubulin
Normalized Expression
p38KbEx41/Ex41
p38KbΔ45/Δ45
G
H
stv
actin
merge
p38KbEx41/Ex41
p38KbΔ45/Δ45
I
stv Localization
Average Pixel Density
p38KbEx41/Ex41
p38KbΔ45/Δ45

Figure 5

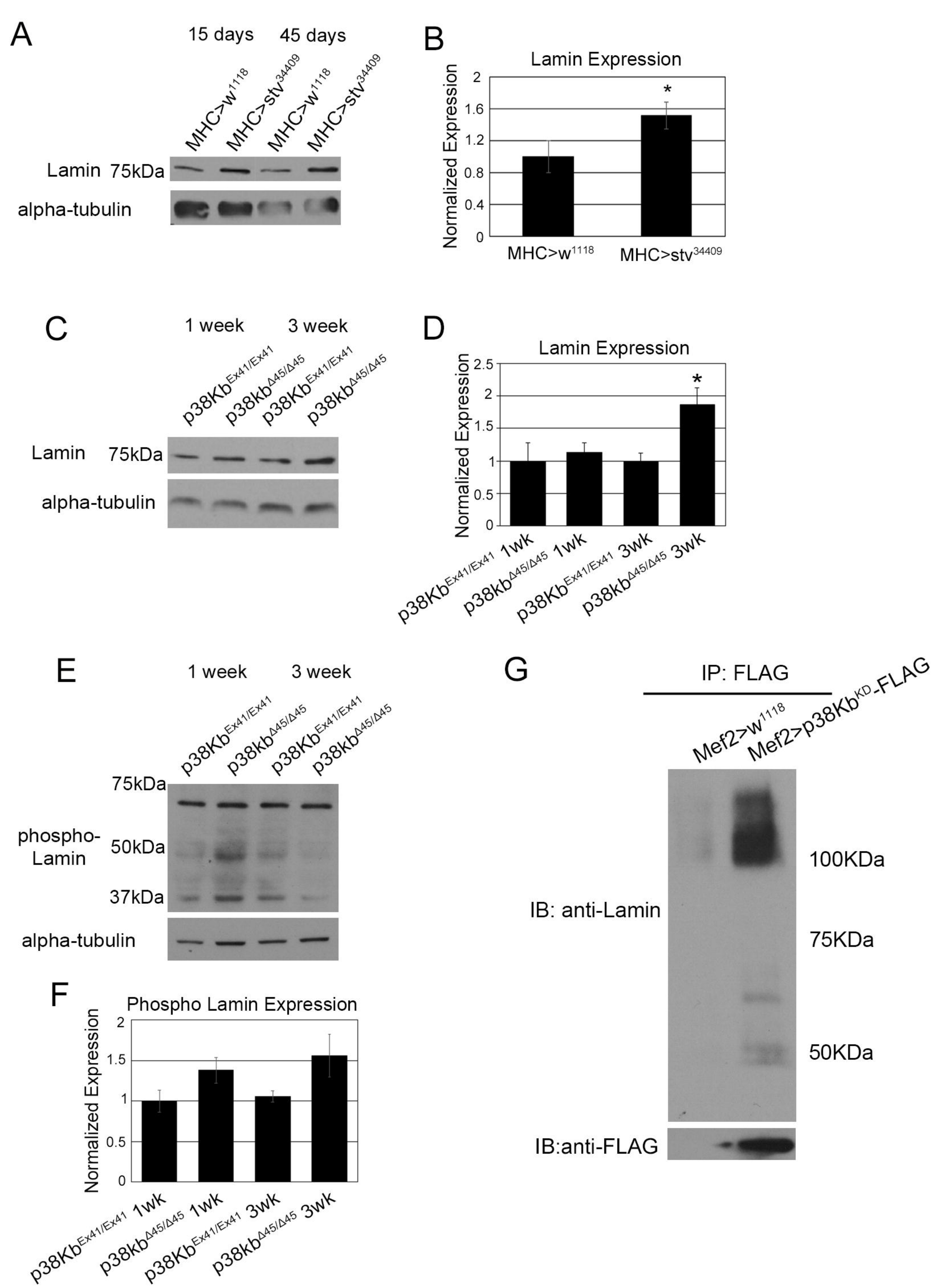
A
15 days
45 days
MHC>w1118
MHC>stv34409
MHC>w1118
MHC>stv34409
Lamin 75kDa
alpha-tubulin
B
Lamin Expression
Normalized Expression
2
1.6
1.2
0.8
0.4
0
*
MHC>w1118
MHC>stv34409
C
1 week
3 week
p38KbEx41/Ex41
p38kbΔ45/Δ45
p38KbEx41/Ex41
p38kbΔ45/Δ45
Lamin 75kDa
alpha-tubulin
D
Lamin Expression
Normalized Expression
2.5
2
1.5
1
0.5
0
*
p38KbEx41/Ex41 1wk
p38kbΔ45/Δ45 1wk
p38KbEx41/Ex41 3wk
p38kbΔ45/Δ45 3wk
E
1 week
3 week
p38KbEx41/Ex41
p38kbΔ45/Δ45
p38KbEx41/Ex41
p38kbΔ45/Δ45
75kDa
phospho-Lamin
50kDa
37kDa
alpha-tubulin
F
Phospho Lamin Expression
Normalized Expression
2
1.5
1
0.5
0
p38KbEx41/Ex41 1wk
p38kbΔ45/Δ45 1wk
p38KbEx41/Ex41 3wk
p38kbΔ45/Δ45 3wk
G
IP: FLAG
Mef2>w1118
Mef2>p38KbKD-FLAG
100KDa
IB: anti-Lamin
75KDa
50KDa
IB:anti-FLAG

Figure 6

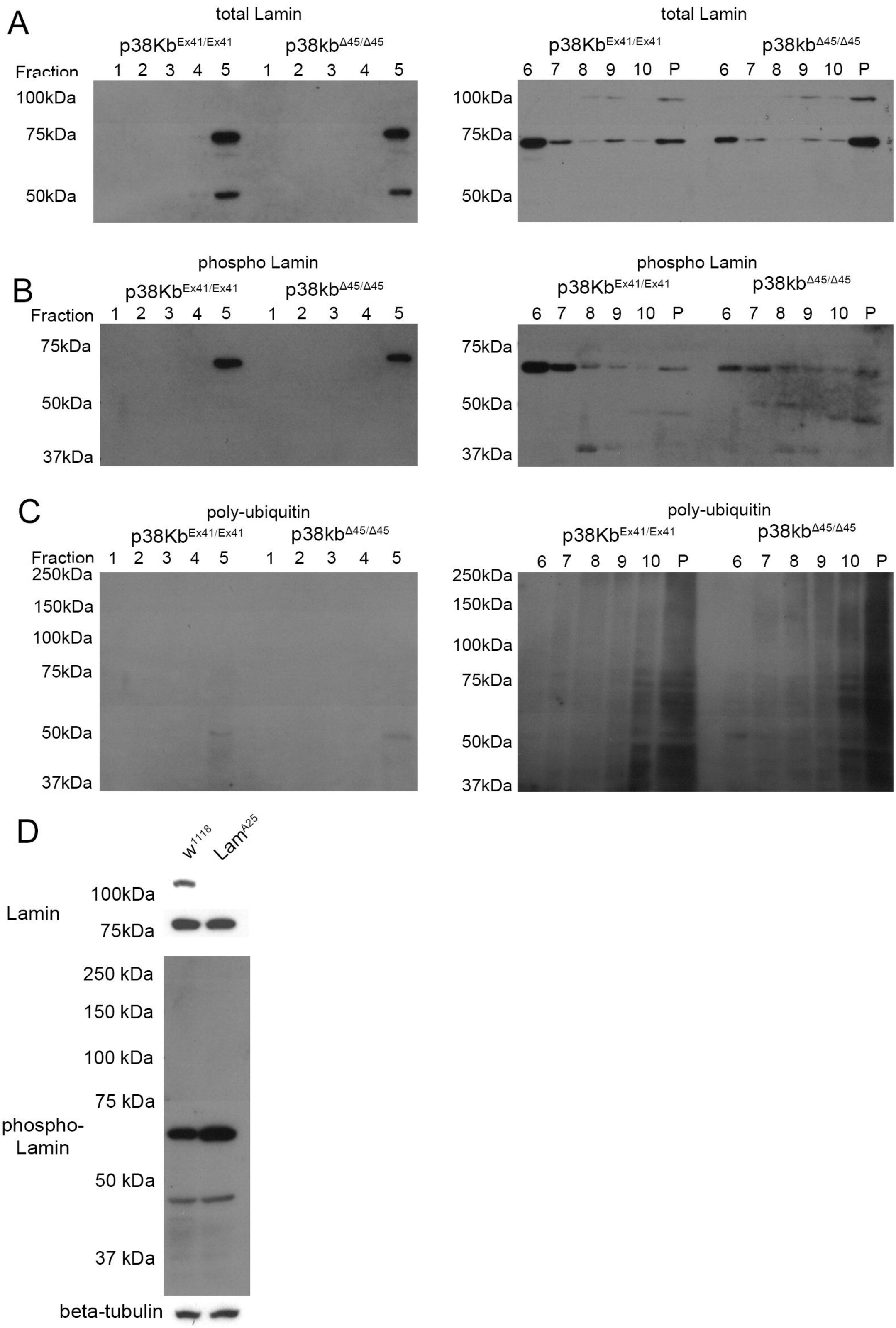
A
total Lamin
p38Kb Ex41/Ex41
p38kb Δ45/Δ45
Fraction 1 2 3 4 5 1 2 3 4 5
100kDa
75kDa
50kDa
total Lamin
p38Kb Ex41/Ex41
p38kb Δ45/Δ45
6 7 8 9 10 P 6 7 8 9 10 P
100kDa
75kDa
50kDa
B
phospho Lamin
p38Kb Ex41/Ex41
p38kb Δ45/Δ45
Fraction 1 2 3 4 5 1 2 3 4 5
75kDa
50kDa
37kDa
phospho Lamin
p38Kb Ex41/Ex41
p38kb Δ45/Δ45
6 7 8 9 10 P 6 7 8 9 10 P
75kDa
50kDa
37kDa
C
poly-ubiquitin
p38Kb Ex41/Ex41
p38kb Δ45/Δ45
Fraction 1 2 3 4 5 1 2 3 4 5
250kDa
150kDa
100kDa
75kDa
50kDa
37kDa
poly-ubiquitin
p38Kb Ex41/Ex41
p38kb Δ45/Δ45
6 7 8 9 10 P 6 7 8 9 10 P
250kDa
150kDa
100kDa
75kDa
50kDa
37kDa
D
w1118
LamA25
Lamin
100kDa
75kDa
250 kDa
150 kDa
100 kDa
75 kDa
phospho-Lamin
50 kDa
37 kDa
beta-tubulin

Figure 7

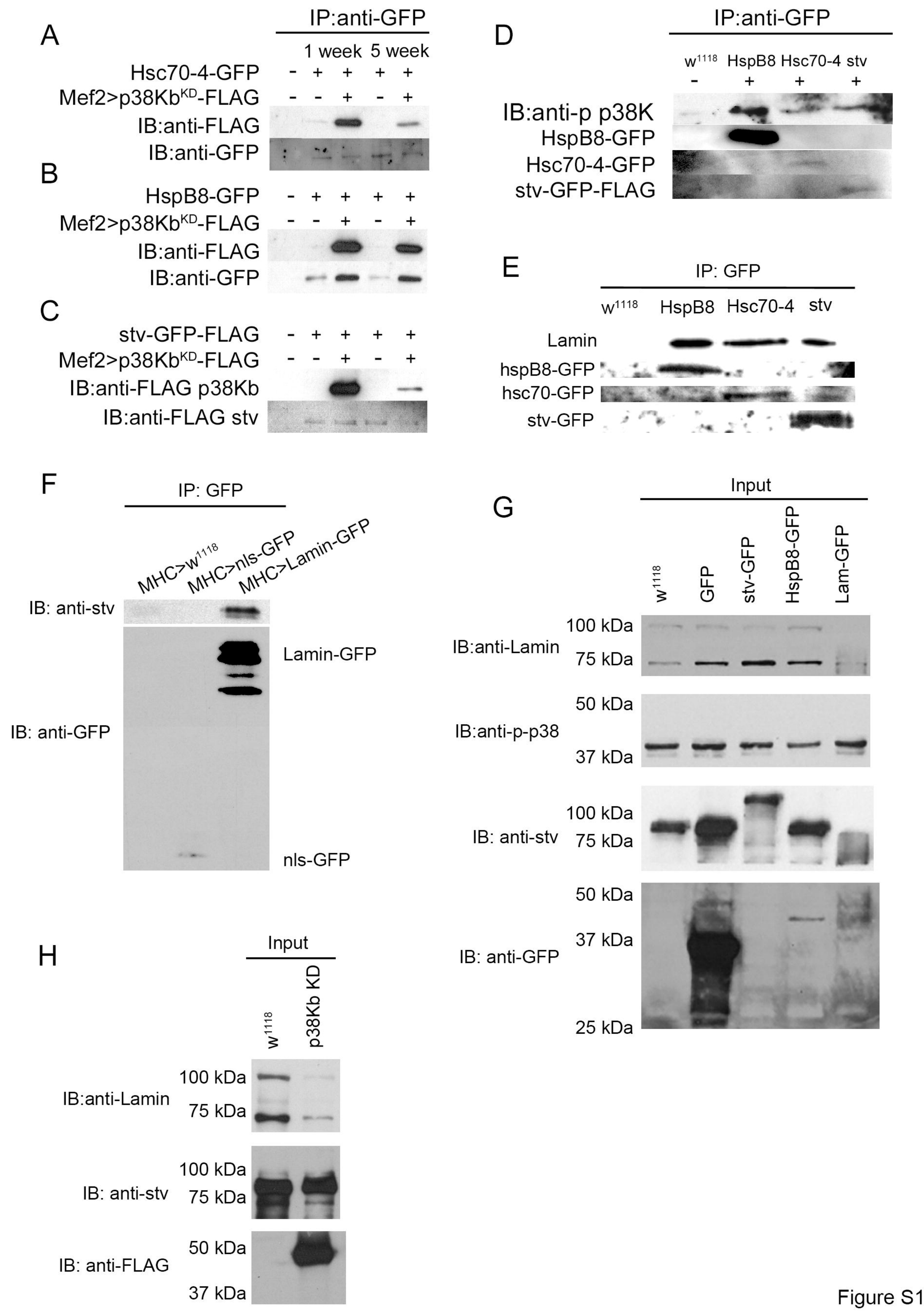
A
IP:anti-GFP
1 week 5 week
Hsc70-4-GFP - + + + +
Mef2>p38Kb^KD-FLAG - - + - +
IB:anti-FLAG
IB:anti-GFP
B
HspB8-GFP - + + + +
Mef2>p38Kb^KD-FLAG - - + - +
IB:anti-FLAG
IB:anti-GFP
C
stv-GFP-FLAG - + + + +
Mef2>p38Kb^KD-FLAG - - + - +
IB:anti-FLAG p38Kb
IB:anti-FLAG stv
D
IP:anti-GFP
w^1118 HspB8 Hsc70-4 stv
- + + +
IB:anti-p p38K
HspB8-GFP
Hsc70-4-GFP
stv-GFP-FLAG
E
IP: GFP
w^1118 HspB8 Hsc70-4 stv
Lamin
hspB8-GFP
hsc70-GFP
stv-GFP
F
IP: GFP
MHC>w^1118
MHC>nls-GFP
MHC>Lamin-GFP
IB: anti-stv
Lamin-GFP
IB: anti-GFP
nls-GFP
G
Input
w^1118
GFP
stv-GFP
HspB8-GFP
Lam-GFP
IB:anti-Lamin
100 kDa
75 kDa
IB:anti-p-p38
50 kDa
37 kDa
IB: anti-stv
100 kDa
75 kDa
IB: anti-GFP
50 kDa
37 kDa
25 kDa
H
Input
w^1118
p38Kb KD
IB:anti-Lamin
100 kDa
75 kDa
IB: anti-stv
100 kDa
75 kDa
IB: anti-FLAG
50 kDa
37 kDa

Figure S1

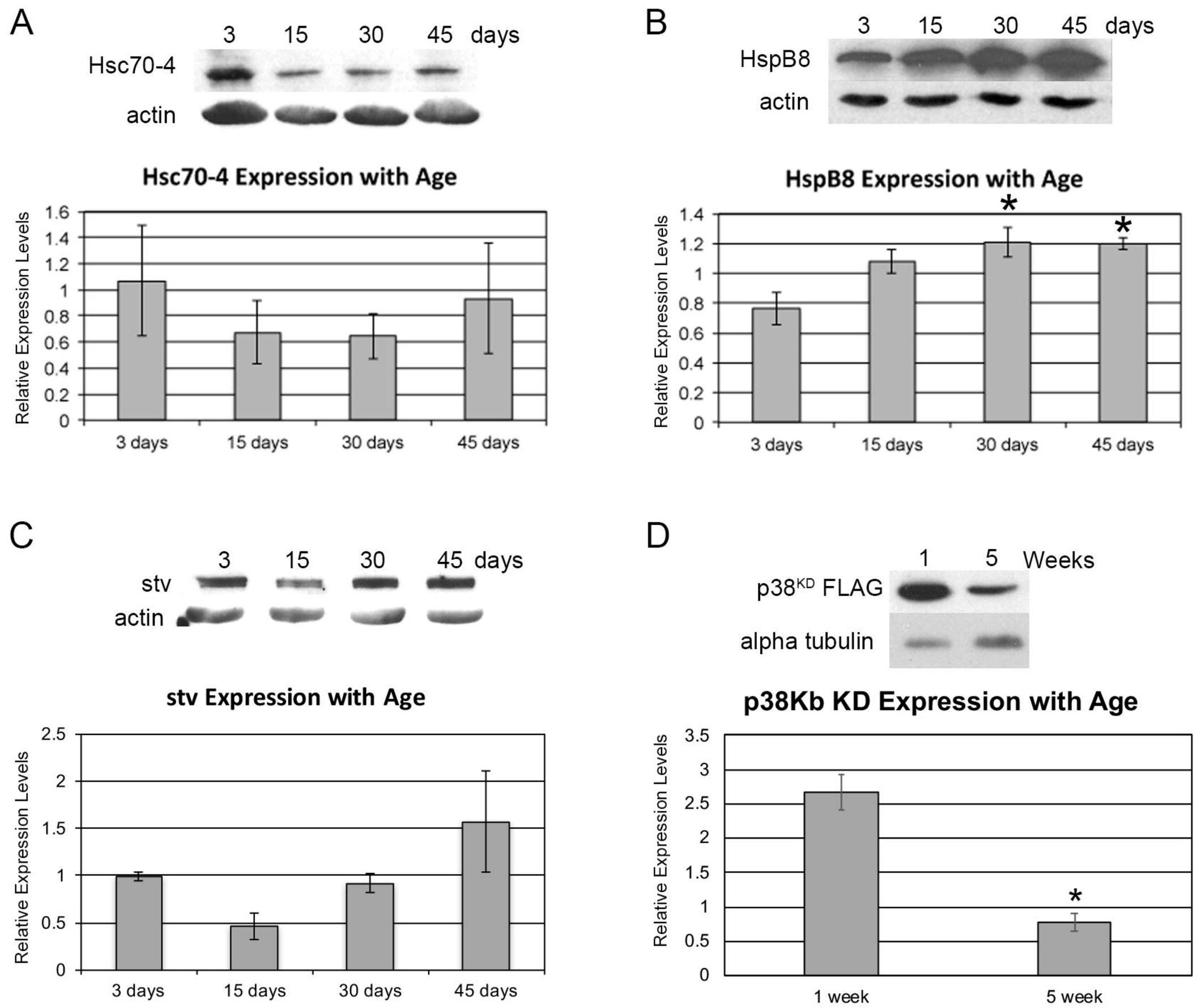
A
3 15 30 45 days
Hsc70-4
actin
Hsc70-4 Expression with Age
Relative Expression Levels
1.6
1.4
1.2
1
0.8
0.6
0.4
0.2
0
3 days
15 days
30 days
45 days
B
3 15 30 45 days
HspB8
actin
HspB8 Expression with Age
Relative Expression Levels
1.4
1.2
1
0.8
0.6
0.4
0.2
0
*
*
3 days
15 days
30 days
45 days
C
3 15 30 45 days
stv
actin
stv Expression with Age
Relative Expression Levels
2.5
2
1.5
1
0.5
0
3 days
15 days
30 days
45 days
D
1 5 Weeks
p38KD FLAG
alpha tubulin
p38Kb KD Expression with Age
Relative Expression Levels
3.5
3
2.5
2
1.5
1
0.5
0
*
1 week
5 week

Figure S2

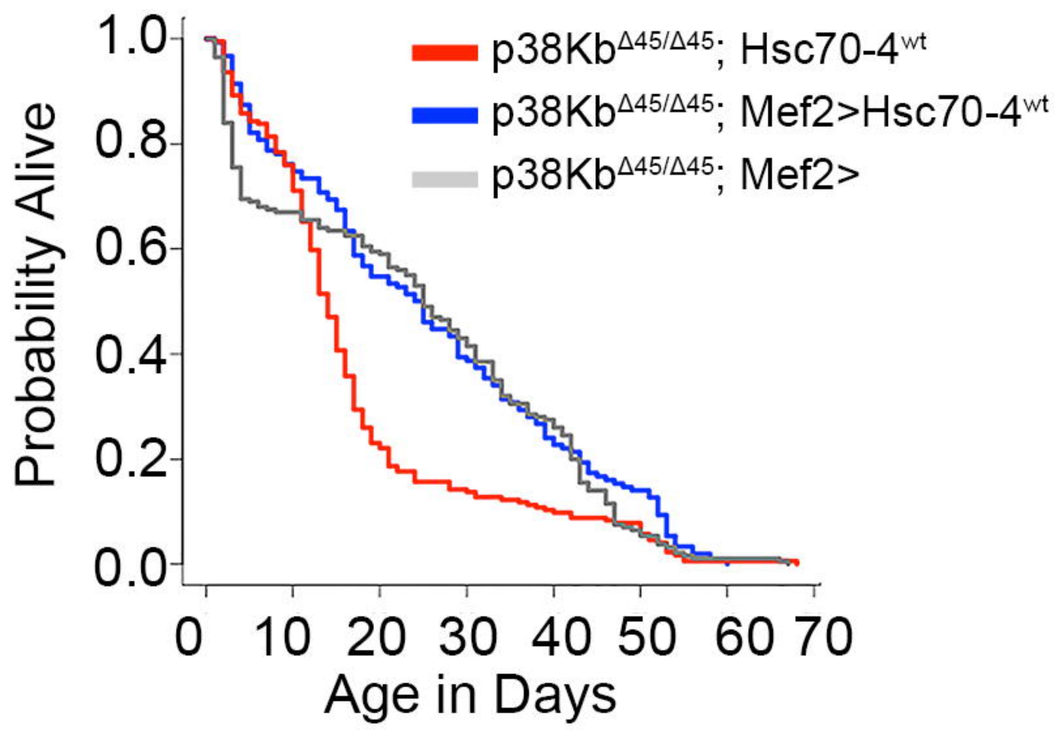
A
Probability Alive
1.0
0.8
0.6
0.4
0.2
0.0
0 10 20 30 40 50 60 70
Age in Days
p38Kb$^{\Delta45/\Delta45}$; Hsc70-4^{wt}
p38Kb$^{\Delta45/\Delta45}$; Mef2>Hsc70-4^{wt}
p38Kb$^{\Delta45/\Delta45}$; Mef2>

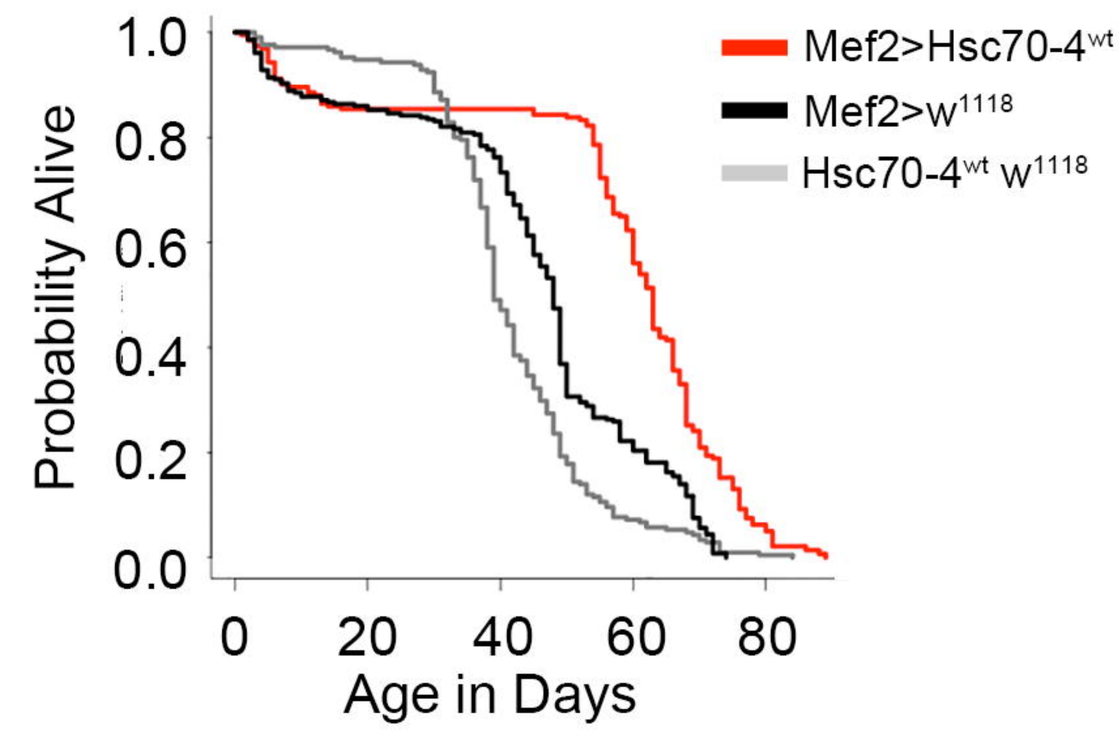
B
Probability Alive
1.0
0.8
0.6
0.4
0.2
0.0
0 20 40 60 80
Age in Days
Mef2>Hsc70-4^{wt}
Mef2>w^{1118}
Hsc70-4^{wt} w^{1118}

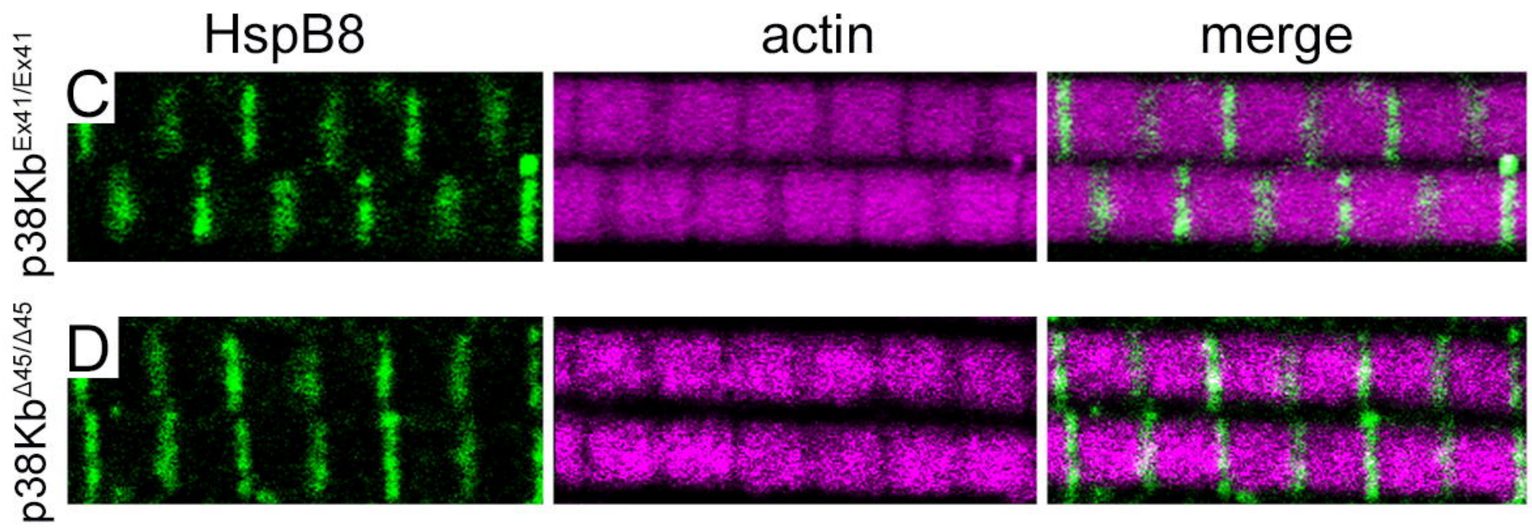
HspB8
actin
merge
C
p38Kb$^{Ex41/Ex41}$
D
p38Kb$^{\Delta45/\Delta45}$

Figure S3